



Carina Elisabeth Ebner, BSc

Strain design and process optimization for the bioreduction of
xylose to xylitol by whole cells of engineered *Saccharomyces*
cerevisiae

MASTER'S THESIS

to achieve the university degree of

Diplom-Ingenieurin

Master's degree programme: Biotechnology

submitted to

Graz University of Technology

Supervisor

Univ.-Prof. Dipl.-Ing. Dr. techn. Bernd Nidetzky

Institute of Biotechnology and Biochemical Engineering

AFFIDAVIT

I declare that I have authored this thesis independently, that I have not used other than the declared sources/resources, and that I have explicitly indicated all material which has been quoted either literally or by content from the sources used. The text document uploaded to TUGRAZonline is identical to the present master's thesis.

Date

Signature

Acknowledgment

I would like to thank Univ.-Prof. Dipl.-Ing. Dr. techn. Bernd Nidetzky, for his supervision, support and for providing me the opportunity to work at the Institute of Biotechnology and Biochemical Engineering.

Special thanks to Mag. rer. nat. Dr. rer. nat. Sarah Pratter, for her support, advice, patience and faith in me. Thank you for going through all that troubles and talking things over with me.

Thanks to Karin Longus and Natascha Loppitsch for their assistance with some experiments. I also would like to thank all the members of the institute, who supported me in the laboratory and encouraged me.

Thanks to WKO Steiermark for the support with a scholarship for my master thesis.

Kurzfassung

Die Aldopentose Xylose ist ein Bestandteil von Harthölzern, aber auch zahlreichen Süßgräsern und Getreidearten. Deshalb stellen land- und forstwirtschaftliche Abfallprodukte eine enorme Xylose-Quelle sowie ein großes ökonomisches Potential für die Xylitolproduktion und die Produktion von Bioethanol dar. Mit steigender Nachfrage nach umweltfreundlicheren und wirtschaftlich preiswerteren Herstellungsverfahren von Xylitol und Ethanol aus Xylose wuchs das Interesse an deren biotechnologischer Herstellung mit Hilfe von Mikroorganismen. Die bevorzugten Xylose-Verwerter darunter sind Hefen. Die Xylose wird mit Hilfe eines geeigneten Enzyms (Xylose Reduktase) zu Xylitol reduziert und ausgeschieden oder tritt nach einem weiteren Oxidationsschritt in den Pentosephosphatweg ein. Unter anaeroben Bedingungen wird der intermediär gebildete Metabolit Pyruvat zu Acetaldehyd decarboxyliert und danach zu Ethanol reduziert. Der Hefe *Saccharomyces cerevisiae* (*S. cerevisiae*) fehlen zwar die maßgebenden Enzyme für den Xylose Abbau, sie gilt aber als gesundheitlich unbedenklich, sehr tolerant gegenüber Inhibitoren und wird daher häufig in der Lebensmittelindustrie oder in der Verarbeitung von Lignocellulose-Hydrolysaten eingesetzt.

Ziel des Projekts ist die Optimierung des biotechnologischen Prozesses zur Herstellung von Xylitol und Bioethanol aus Xylose. Die Bedeutung des Xylose-Transports in diesem Prozess wird untersucht in dem Xylose-spezifische Transportproteine in ausgewählte *S. cerevisiae* Stämme eingebracht werden, die in der Lage sind Xylose zu Xylitol bzw. Ethanol umzuwandeln. Stellt die Xylose-Aufnahme tatsächlich einen limitierenden Faktor in den Elternstämmen dar, könnte mit den entwickelten Stamm-Varianten eine enorme Produktivitätssteigerung erreicht werden. Eine gesteigerte Xylitolproduktionsrate durch einen gezielt veränderte *S. cerevisiae* Stamm ist ein großer Schritt in Richtung umweltfreundlicher Biosynthese von Xylitol/Bioethanol und legt den Grundstein für eine effiziente und nachhaltige Produktion im großindustriellen Maßstab.

Abstract

S. cerevisiae has been extensively studied with regards to its biotechnological application in the production of xylitol and ethanol from xylose, which is present in lignocellulosic hydrolysates. Besides several potential limitations in the recombinant xylose utilization pathways, substrate transport into the cell is suggested to be one of the major bottlenecks. *S. cerevisiae* sugar transporters take up hexoses, another component of lignocellulosic hydrolysates, by facilitated diffusion. Xylose is incorporated by the same transporters however, the pentose is shuttled at a much lower rate and with an affinity that is in many cases two orders of magnitude lower than that for glucose. A few proteins that are present in natively xylose converting microorganisms or *S. cerevisiae* transporters that were engineered for xylose uptake have been experimentally identified to show a preference of xylose transport over glucose transport. This property makes them interesting candidates for studies on microbial xylose uptake. The goal of this work was to determine and compare the effect of two selected transporters, Gal2_N376F and Xut1, in regard to xylose consumption and xylitol or ethanol production in recombinant *S. cerevisiae*. So far investigated glucose/xylose transporters were mostly characterized in yeast strains that lacked endogenous sugar-transporters. The current study aimed at a more applicable approach: providing information about the profitability of recombinant transporter expression in strains that possess their functional transporter system.

Table of Contents

1	Introduction	8
2	Materials and Methods	14
2.1	Chemicals	14
2.2	Cultivation media, buffers and solutions	14
2.2.1	<i>Escherichia coli</i> media	14
2.2.2	<i>Saccharomyces cerevisiae</i> media	14
2.2.3	Buffers and solutions	15
2.3	Strains, plasmids and genes	16
2.3.1	Used strains	16
2.3.2	Used plasmids	16
2.3.3	Used genes	16
2.4	Cloning	17
2.4.1	Polymerase chain reactions (PCR)	17
2.4.2	Restriction digest and dephosphorylation of vector DNA	21
2.4.3	Ligation of DNA fragments	21
2.4.4	Transformation (and isolation) of plasmid DNA	22
2.5	Construction of yeast reference strains and strains, expressing the Gal2_N376F or XUT1 transporter.	23
2.5.1	Construction of the reference strains <i>S. c.</i> XR (g)-p427TEF, <i>S. c.</i> XR (2 μ)-p427TEF and <i>S. c.</i> IBB10B05-p427TEF	23
2.5.2	Construction of strains, expressing the Gal2_N376F transporter	23
2.5.3	Construction of strains, expressing the XUT1 transporter	24
2.6	Xylose fermentations	26
2.6.1	(Semi-)aerobic fermentations in shaking flasks	26
2.6.2	Anaerobic fermentations	27
2.7	Analytical methods	27
2.7.1	Protein analytics	27
2.7.2	Determination of XR activity in cell free extracts	29
2.7.3	Analysis of fermentation products (HPLC measurements)	29
2.7.4	Determination of growth rates	30

2.7.5	Determination of yields	30
2.7.6	Determination of xylose uptake rates and xylitol or ethanol productivities	30
3	Results and Discussion	31
3.1	<i>E. coli</i> subcloning and <i>S. cerevisiae</i> transformation	31
3.2	XR activities in recombinant <i>S. cerevisiae</i> strains	34
3.3	The effect of xylose transporter expression in a xylitol-producing low-XR-activity strain	37
3.4	The effect of xylose transporter expression in a xylitol-producing high-XR-activity strain	40
3.5	The effect of xylose transporter expression in an ethanol-producing high-XR-activity strain	47
3.6	Analysis of Gal2_N376F transporter expression	52
4	Conclusion	56
5	References	57
6	Appendix	62
6.1	DNA and Protein Sequences	62
6.2	Batch Conversion Diagrams	65
6.3	Instruments and devices	66

1 Introduction

The aldopentose D-xylose (all sugar mentions refer to the D-enantiomer; the descriptor “D-” is omitted from now on) is one of the most abundant sugars in nature. It is the major building block of the hemicellulose fraction in lignified plants and accounts for up to 80% of the sugar content in hemicellulose [1]. Monomeric xylose is obtained from chemically [2] or biologically [3] processed hardwood hydrolysates using chipping, steam explosion or other mechanical methods in combination with acid pretreatment [4]. Its ubiquity and renewability make xylose an interesting raw material for the sustainable production of different chemicals or biofuels.

A highly valuable bulk product that can be obtained from xylose is xylitol. Xylitol is a five-carbon sugar alcohol, found in various fruits and vegetables. However, its extraction from such sources is uneconomical because of the low quantities that are usually obtained. Xylitol equals the sweetness of sucrose, but has a lower energy value (2.4 kcal/g vs 4.0 kcal/g) [5]. In addition to its suitability for insulin-deficient patients it possesses anticariogenicity and remineralization properties [6]. Due to these beneficial effects xylitol has become a globally used sweetener which is often added to foods and personal care products. Industrially, xylitol is produced by catalytic hydrogenation of xylose in the presence of a Raney nickel catalyst [6] under high temperature (80-140°C) and pressure (< 50 bar). Additionally, several expensive purification steps are required because only pure xylose can be used for chemical reduction [7, 8]. In contrast, xylitol production through microbial bioconversion of xylose-containing undetoxified lignocellulosic hydrolysates is possible [9, 10]. Not surprisingly, with increasing interest in environmentally friendly and economically more beneficial xylitol production methods, the biosynthesis of xylitol using microorganisms became more popular [8].

Another large field, that employs microorganisms for xylose utilization is the biofuel sector. The limited source of fossil energy and the dependence on crude oil as raw material for bulk and fine chemicals as well as transport fuels during the last decade created a predominant need for alternative energy sources [11]. Biofuel production from plant biomass hydrolysates is a promising alternative for sustainable energy supply and therefore of great economic and environmental significance. The economical production of second-generation bio-ethanol requires effective conversion of all the sugars in lignocellulosic raw material hydrolysates into ethanol [12]. The demands on the microorganisms that perform this biosynthesis are the ability of effective metabolization of

lignocellulosic biomass, strong tolerance against inhibitors that are present in the hydrolysates as well as against high concentrations of ethanol.

Among the microorganisms employed for xylose utilization, yeasts are the preferred biocatalysts. The majority of yeasts and fungi convert xylose to xylulose in two steps. First, xylose is reduced by the NADH- or NADPH-dependent xylose reductase (XR). The resulting xylitol can be secreted or, in a second step, further oxidized to xylulose by an NAD⁺-dependent xylitol dehydrogenase (XDH) [8]. The product xylulose is further metabolized to xylulose-5-phosphate by xylulokinase (XKS). Xylulose-5-phosphate subsequently enters the pentose phosphate pathway (PPP) where it is channeled into glycolytic intermediates such as glyceraldehyde-3-phosphate and fructose-6-phosphate. These intermediates are converted to pyruvate in the Emden-Meyerhof-Parnas pathway. Under anaerobic conditions, pyruvate is decarboxylated by pyruvate decarboxylase to acetaldehyde which is then reduced to ethanol by alcohol dehydrogenase [13].

Yeasts have been extensively studied with regards to their biotechnological application in the production of xylitol and ethanol [10, 14–16]. While *Candida spp.* are natural xylose consumers, *S. cerevisiae*, the most commonly used yeast in industrial applications [17], lacks the xylose metabolic pathway [18]. Nevertheless, biotechnological long-term experiences with baker's yeast, its GRAS (generally recognized as safe) status and strong tolerance against inhibitors present in lignocellulosic hydrolysates attracted researchers attention. Therefore, recombinant *S. cerevisiae* strains were constructed by the introduction of genes that are required for xylose utilization [16, 19–21]. However, strain engineering suffers from several bottlenecks: enzyme activities play a key role in the fermentation process [13, 14, 20], but also cofactor regeneration and availability are crucial factors. The opposite cofactor specificities of XR and XDH cause redox imbalances in the cell and have to be overcome in biocatalysts employed for ethanol production [20, 22].

Another major limitation in xylose utilization can be the substrate uptake into the cell. It has been demonstrated or inferred in several cases that pentose transport accounts for significant pathway flux control [23, 24]. Transport is a bottleneck in xylose fermentation, at least at low concentrations, and certainly with improvements of intracellular xylose metabolism the impact of this limitation increases [24–26]. The degree to which transport controls xylose utilization depends on the flux in the downstream pathway which is in turn dependent on the strain background (fast or slow xylose catabolism) [27, 28]. Thus, one approach to increase the efficiency of *S. cerevisiae*-catalyzed conversion of xylose is to enhance its uptake by the yeast.

S. cerevisiae possesses monosaccharide transporters that operate by facilitated diffusion, an energy-independent mechanism that catalyses the movement of a single solute molecule at a time down its concentration gradient, across a membrane. Other transporters, which usually operate only when the amount of sugar in the medium is scarce, are energy-consuming systems that are able to transport a solute against its concentration gradient, coupled to the simultaneous movement of (a) proton(s). The vast majority of *S. cerevisiae* sugar transporters takes up hexoses by facilitated diffusion [29, 30]. Xylose is transported by the same system but at a much lower rate and with an affinity that is in many cases two orders of magnitude lower than that for glucose [17, 31]. Given that pretreated and enzymatically processed cellulosic and hemicellulosic materials contain a mixture of several sugars including glucose, xylose, mannose, galactose, and arabinose, xylose uptake and utilization is impaired by the presence of the competing sugars and mainly prevented until glucose is consumed from the fermentation broth. Especially in xylitol production, where a co-substrate (preferably glucose) is needed for generation of maintenance energy, simultaneous consumption of glucose and pentoses is the major obstacle for efficient and fast xylose fermentation [25]. Additionally, when the substrate includes large initial concentrations of glucose, fermentation may result in inhibitory concentrations of produced ethanol before xylose uptake begins. Taken together, a xylose transporter that is not inhibited by glucose is a vital prerequisite for fermentation of substrates containing glucose and xylose [17, 25].

Several studies suggest that the expression of heterologous transporters can improve *S. cerevisiae* xylose fermentation characteristics [17, 25] and native pentose-utilizing microorganisms are considered to be good sources of such carriers [23, 29, 32]. Many heterologous hexose/pentose transporters have been expressed and studied in *S. cerevisiae* [28, 32–36]. Weierstall *et al.* identified three genes, called *SUT1-3*, encoding glucose transporters in the yeast *Pichia stipitis* (*P. stipitis*). Their kinetic characterization in *S. cerevisiae* revealed all of them to be specific for glucose (K_m values of 0.8 – 1.5 mM) and to be able to transport xylose, but with a very low affinity (K_m values of 49 – 145 mM) [37]. Leandro *et al.* discovered the high affinity xylose/glucose symporter Gxs1 and the low affinity xylose/glucose facilitator Gxf1 from *Candida intermedia* (*Ci*). It was observed that the overexpression of the Gxf1 transporter improved the fermentation performance in a recombinant *S. cerevisiae* strain and that the V_{max} of xylose transport of Gxs1 ($V_{max} 6.5 \pm 1.5 \text{ nmol}/(\text{min} \cdot \text{mg}_{CDW})$) was one order of magnitude lower when compared with Gxf1 [31, 35]. In addition, Runquist *et al.* demonstrated that the heterologous expression of the Gxf1 transporter increased the overall xylose transport performance by 3.9-fold ($V_{max} 471 \pm 10 \text{ nmol}/(\text{min} \cdot \text{mg}_{CDW})$) compared to a control strain ($V_{max} 119 \pm 17 \text{ nmol}/(\text{min} \cdot \text{mg}_{CDW})$), whereas the expression of Sut1 transporter ($V_{max} 178 \pm 16$

nmol/(min*mg_{CDW})) only slightly improved the xylose utilization rate [27, 28]. The high differences of the V_{\max} values mentioned above are a matter of different methods of determination. Runquist *et al.* measured the overall cellular transport capacity of strains that expressed all the native transporters, whereas Leandro *et al.* used strains that lacked all native hexose transporters. The slight improvement of xylose utilization, when using a *S. cerevisiae* strain expressing Sut1 transporter, was also seen in the study of Katahira *et al.* Both the specific xylose consumption rate and specific ethanol productivity (0.23 g_{xyI}/(g_{CDW}*h) and 0.072 g_{ETOH}/(g_{CDW}*h)) were higher in the initial phase compared to the control strain (0.20 g_{xyI}/(g_{CDW}*h) and 0.057 g_{ETOH}/(g_{CDW}*h)), when a large amount of xylose was present [34]. *S. cerevisiae* strains overexpressing heterologous transporters from *Arabidopsis thaliana* (*A. thaliana*) AT5g59250 and At5g17919 also showed up to 2.5-fold enhanced xylose consumption compared to the control strain [31, 33]. Unfortunately, different strain backgrounds and experimental setups prevent direct comparison of several studies. Additionally to the investigations on heterologous hexose/pentose transporters, the endogenous hexose transporters Hxt1-17 and Gal2 of *S. cerevisiae* were characterized [25, 36, 38, 39]. Xylose uptake rates investigated by Hamacher *et al.* were highest for Hxt7 (48 nmol/(min*mg_{CDW})) and lowest for Hxt5 (11 nmol/(min*mg_{CDW})). Besides the determination of xylose uptake activities via [¹⁴C]-labeled xylose uptake assays, it was also investigated if the transporters confer growth to strains that lack the native hexose transporters. It was demonstrated that some native hexose transporters, Hxt4, Hxt5, Hxt7 and Gal2, were able to support growth on xylose (2%) [38]. The endogenous hexose transporters Hxt7 conferred growth with a rate of $0.09 \pm 0.02 \text{ h}^{-1}$ and Gal2 showed a growth rate (μ) of $0.112 \pm 0.02 \text{ h}^{-1}$ [36]. However, the low-affinity hexose transporters Hxt1, Hxt3 and also the very weakly expressed transporters Hxt8 and Hxt17 were not able to transport xylose, at least not in amounts sufficient to support growth [38]. Furthermore, the heterologous transporters Gxf1 (μ $0.070 \pm 0.003 \text{ h}^{-1}$), Gxs1 (μ $0.049 \pm 0.004 \text{ h}^{-1}$), Xut1 (μ $0.050 \pm 0.001 \text{ h}^{-1}$) and Xut3 (μ $0.0570 \pm 0.005 \text{ h}^{-1}$) were also shown to confer growth on 20 g/L xylose [36, 40, 41].

From all the mentioned transporters only the Xut1 permease [17], showed a preference of xylose transport over glucose transport in *S. cerevisiae*, which makes it interesting for further studies. The Xut1 transporter of *P. stipitis* has been shown to have a 2-fold lower K_m value for xylose (0.46 mM) than for glucose (0.91 mM), resulting in a significantly higher affinity for the pentose [17]. However, to date the pentose uptake capacity using heterologous transporters is still low. The main challenge remains the contradiction between the enhanced xylose specificity but still often very low efficiency of xylose transport, due to competitive inhibition of glucose [32]. Molecular modifications on heterologous or endogenous transporters altered their xylose transport performance, especially

when glucose was present. For example, an *S. cerevisiae* endogenous transporter mutant, the galactose permease Gal2_N376F [25], was found to increase xylose transport preference by 2.4-fold. The functional study results showed that glucose did not inhibit the transport of xylose by Gal2_N376F. The transporter had a high affinity for xylose along with a moderate transport velocity (V_{\max} 37.3 ± 1.3 nmol/(min*mg_{CDW})) [25, 32]. A summary of studied xylose transporters and the according kinetic data is given in Table 1.

The goal of this study was the evaluation and comparison of two xylose transporters in regard to their effect on xylitol or ethanol production in recombinant *S. cerevisiae*. So far investigated glucose/xylose transporters were mostly characterized in yeast strains that lacked endogenous sugar-transporters [17, 25, 32, 36, 42]. The present work aimed at providing information about the suitability of recombinant transporter expression in strains that possess an intact native transporter system. From the variety of known representatives, the Gal2_N376F transporter was chosen because of its inability to take up glucose and its comparably low K_m for xylose (91.4 ± 8.9 mM). The Xut1 transporter was chosen because of its lower K_m value for xylose (0.46 ± 0.02 mM) than for glucose (0.91 ± 0.01 mM) and its high xylose uptake specificity ($V_{\max}/K_m = 252.2$ min⁻¹) (Table 1). The proteins were expressed in three differently engineered *S. cerevisiae* strains using high-copy plasmids. Biocatalysts were then subjected to batch conversions using commercially available xylose and, if required, different co-substrates. Strains containing the *Candida tenuis* (Ct) XR only were evaluated based on xylose uptake rates, xylitol productivities, xylitol yields and co-substrate yields. The performance of the strain carrying a full xylose utilization pathway consisting of CtXR, *Galactocandida mastotermitis* (Gm) XDH and *S. cerevisiae* XKS1 was assessed by determining the xylose uptake rates as well as ethanol yields. Results were compared and the impact of the different transporters on xylose utilization properties of *S. cerevisiae* is discussed.

Table 1: Summary of kinetic data of hexose/pentose transport proteins studied in *S. cerevisiae* strains. Endogenous *S. cerevisiae* transporters are marked light grey; Dark gray marked transporters were chosen for this study

Transporter	Km [mM]		V _{max} [nmol/(min*mg _{CDW})]		Specificity V _{max} / Km [min ⁻¹]		Ref.
	Glucose	Xylose	Glucose	Xylose	Glucose	Xylose	
<i>PsSut1</i>	1.5 ± 0.1	145 ± 1.0	45 ± 1.0	132 ± 1.0	30	0.9	[37]
<i>PsSut2</i>	1.1 ± 0.1	49.0 ± 1.0	3.3 ± 0.1	28 ± 4.0	3.3	0.6	[37]
<i>PsSut3</i>	0.8 ± 0.1	103 ± 3.0	3.7 ± 0.1	87 ± 2.0	4.6	0.8	[37]
<i>PsSut4</i>	1.3 ± 0.1	16.6 ± 0.3	105 ± 4.2	122 ± 2.4	80.8	7.4	[17]
<i>CiGxf1</i>	2.0 ± 0.6	48.7 ± 6.5	~ 163	~ 25	81.5	0.5	[17, 35]
<i>ScHxt1</i>	(a) 107 ± 49	(b) 880 ± 6.5	(a) 50.9 ± 3.7	(b) 750 ± 94	0.5	0.8	a [43] b [42]
<i>ScHxt2</i>	(a) 2.9 ± 0.3	(b) 260 ± 130	(a) 15.6 ± 0.9	(b) 340 ± 10	5.4	1.3	a [43] b [42]
<i>ScHxt3</i>	(a) 107 ± 49	(b) 880 ± 6.5	(a) 50.9 ± 3.7	(b) 750 ± 94	0.5	0.8	a [43] b [42]
<i>ScHxt4</i>	(a) 6.2 ± 0.5	(b) 170 ± 120	(a) 12.0 ± 0.9	(b) 190 ± 23	1.9	1.1	a [43] b [42]
<i>ScHxt7</i>	0.5 ± 0.1	200.3 ± 13.2	26.0 ± 1.1	67.0 ± 2.0	52	0.3	[25]
<i>ScGal2</i>	1.5 ± 0.2	225.6 ± 15.8	27.2 ± 0.9	93.1 ± 3.2	17.5	0.4	[25]
<i>ScGal2_</i> <i>N376F</i>	n. d.	91.4 ± 8.9	b. d.	37.3 ± 1.3	-	0.4	[25]
<i>CiGxs1</i>	0.012 ± 0.004	0.4 ± 0.1	4.3 ± 0.33	6.5 ± 1.5	358.3	16.2	[35]
<i>PsXut1</i>	0.91 ± 0.01	0.46 ± 0.02	80 ± 1.0	116 ± 5.8	87.91	252.2	[17]

b. d. = below detection limit; n. d. = not determinable;

2 Materials and Methods

2.1 Chemicals

If not otherwise stated the chemicals and antibiotics used in this study were of analytical grade and purchased from Carl Roth (Karlsruhe, Germany). Primers, SD medium lacking uracil, ergosterol, antifoam 204, SS-carrier DNA, and PEG 3640 were from Sigma Aldrich (St. Louis, USA). Polymerases, restriction enzymes, T4 DNA Ligase and Fast Alkaline Phosphatase were from Thermo Scientific – Life Technologies (Waltham, USA).

2.2 Cultivation media, buffers and solutions

All media and buffers were prepared in ultra-pure, deionized water (ddH₂O). All media were autoclaved at 121°C for 20 minutes. For the preparation of agar plates, the respective medium was supplemented with 15 g/L agar before sterilization.

2.2.1 *Escherichia coli* media

LB (Luria Bertani): 10 g/L peptone, 5 g/L yeast extract, 10 g/L NaCl. If needed, 1000-fold concentrated antibiotic stock solutions were prepared, filter-sterilized, and added to the medium after autoclaving and cooling down to ~50°C to give final concentrations of 100 µg/mL ampicillin or 50 µg/mL kanamycin.

SOC: 20 g/L peptone, 0.58 g/L NaCl, 5 g/L yeast extract, 0.18 g/L KCl, 2.46 g/L MgSO₄, 3.81 g/L glucose monohydrate.

2.2.2 *Saccharomyces cerevisiae* media

YP: 10 g/L yeast extract and 20 g/L peptone.

Synthetic drop-out (SD) medium: 1.7 g/L yeast nitrogen base lacking amino acids and (NH₄)₂SO₄, 1.9 g/L yeast SD medium lacking uracil.

YPD: YP medium with 20 g/L glucose, which were added after autoclaving.

SDD: SD medium with 20 g/L glucose, which were added after autoclaving.

SDE: SD medium with 9.2 g/L ethanol which were added after autoclaving.

Mineral medium (M- medium): 5 g/L $(\text{NH}_4)_2\text{SO}_4$, 0.5 g/L $\text{MgSO}_4 \cdot 7\text{H}_2\text{O}$, 0.42 mg/L Tween-80, 10 mg/L ergosterol, 250 $\mu\text{L/L}$ antifoam 204, trace elements and vitamins [44, 45] and 14.4 g/L K_2HPO_4 . Ergosterol was used only for conversions with xylose.

The pH of all *S. cerevisiae* media was set to 6.5 prior to sterilization. If needed, a 250-fold antibiotic stock solution was prepared, filter sterilized, and added to the media after autoclaving and cooling down to $\sim 50^\circ\text{C}$ to give a final concentration of 200 $\mu\text{g/mL}$ geneticin-sulfat.

2.2.3 Buffers and solutions

100 mM PPB: 13.92 g/L K_2HPO_4 and 2.69 g/L KH_2PO_4 , pH 7.5. The buffer was autoclaved before use.

50x TAE: 242 g/L Tris, 57.1 g/L acetic acid, 18.6 g/L EDTA.

MOPS Buffer (20X): NuPage® Thermo Scientific

Coomassie staining solution: 2.5 g brilliant blue G250, 500 mL ethanol, 75 mL acetic acid set to an end volume of 1 L with ddH₂O.

Destaining solution: 75 mL acetic acid, 200 mL ethanol set to an end volume of 1 L with ddH₂O.

10x Tris Glycine Transfer Buffer: 140 g glycine, 30 g Tris dissolved in ddH₂O and set to a final volume of 1 liter.

1x Tris Glycine Transfer Buffer: 100 mL of 10x Tris Glycine Transfer Buffer mixed with 200 mL of methanol and 700 mL of ddH₂O.

1x PBS: 137 mM NaCl, 10 mM Na_2HPO_4 , 2.7 mM KCl, 1.8 mM KH_2PO_4 , pH 7.4.

Blocking Solution: 3% Bovine Serum Albumine, 0.5% TWEEN20® dissolved in 1x PBS

PBST: 0.1% v/v TWEEN20® dissolved in 1x PBS

SS-carrier DNA: Deoxyribonucleic acid, single stranded from salmon testes [10 mg/mL] was diluted with sterile ddH₂O to a final concentration of 2 mg/mL.

Polyethylene glycol (PEG) 3640 50% (w/v): 5 g PEG 3640 were carefully dissolved in ddH₂O and set to an end-volume of 10 mL. The solution was sterile-filtered.

Lithium acetate 1 M: 2.64 g lithium acetate were dissolved in 35 mL ddH₂O and set to an end-volume of 40 mL. The pH was adjusted to 7.5 with acetic acid.

2.3 Strains, plasmids and genes

2.3.1 Used strains

E. coli TOP10 and *E. coli* DH5 α were used as bacterial hosts for sub-cloning. The parental yeast strains used in this study were *S. cerevisiae* CEN.PK 113-7D (MATa MAL2-8c SUC2) (termed *S. c.* wild-type) and *S. cerevisiae* CEN.PK 113-5D (*S. cerevisiae* CEN.PK 113-7D-URA; MATa MAL2-8c SIC2 *ura3*) with a genome-integrated expression cassette encoding the *CtXR* enzyme (termed *S. c.* XR (g)). Additionally, a recombinant *S. cerevisiae* strain with the gene encoding *CtXR* on the yeast 2 μ expression plasmid p426GPD was used. This strain is termed *S. c.* XR (2 μ). Furthermore the strain *S. c.* IBB10B05 (CEN.PK 113-5D; MATa MAL2-8c SIC2 *ura3*) with a genome integrated expression cassette encoding the *CtXR* (K274R/N276D double mutant form), *GmXDH* and *S. cerevisiae* XKS1, that is capable of ethanol production with xylose as the only substrate, was tested. The strains were provided by the Institute of Biotechnology and Biochemical Engineering, Graz University of Technology [21, 46].

2.3.2 Used plasmids

The expression plasmid used in this study was p427TEF. The vector card is displayed in Figure 1.

2.3.3 Used genes

The gene of *Xut1* was ordered, flanked with the restriction sites *Bam*HI and *Xma*I on the 5'- and 3'-end, respectively, from Eurofins Genomics (Germany) and it was delivered in the pEX-K4 plasmid. The gene of the Gal2_N376F permease mutant [25] was ordered with restriction sites for *Xma*I (5'-end) and *Eco*RI (3'-end) from GenScript Corporation, Piscataway, NJ, USA and arrived in the pUC57-Kan plasmid. The DNA- and protein sequences of the transporters can be found in the Appendix (section 6.1).

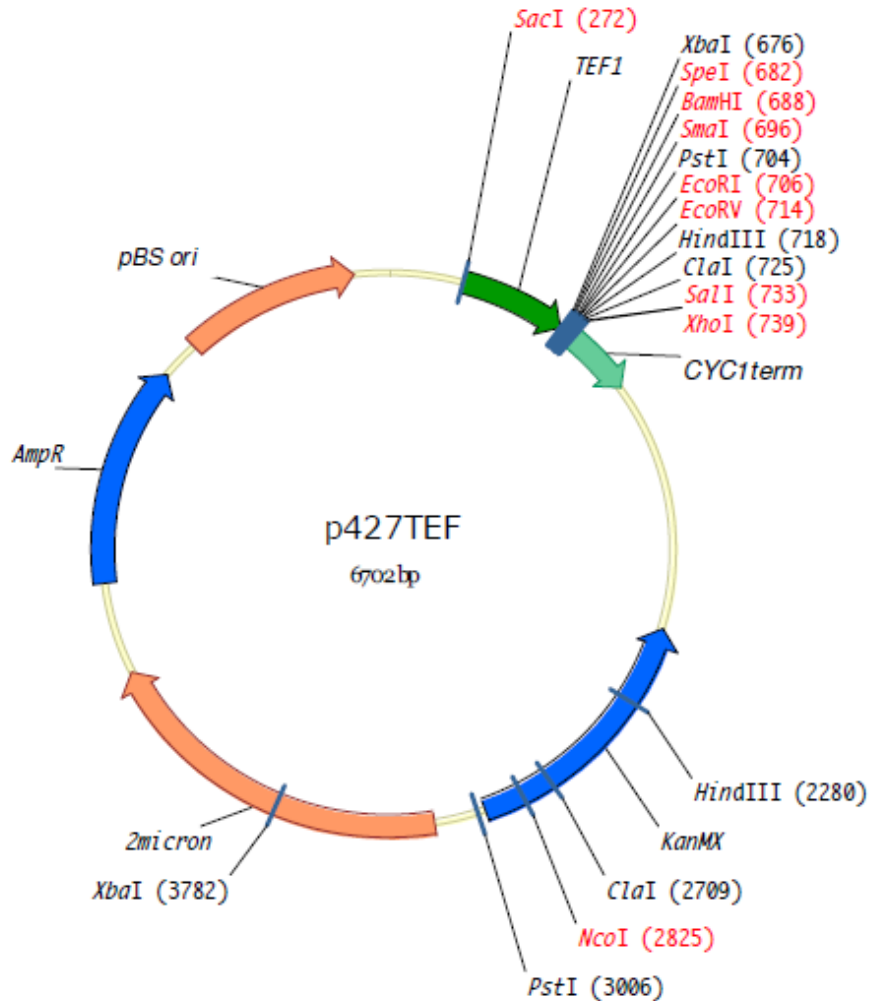


Figure 1: p427TEF expression vector: TEF1 promoter: Transcription factor TEF drives strong, constitutive expression; MCS (675 – 743): Multiple cloning site containing different restriction sites; CYC1term: cytochrome-c-oxidase terminator (CYC1_T); KanMX: Kanamycine resistance gene conferring kanamycine (30 µg/mL) resistance in *E. coli* and Geneticin-Sulfat (200 µg/mL) in *S. cerevisiae*; 2micron: origin of replication, allows propagation of plasmid in yeast at high copy numbers (20-100 copies/cell); AmpR: ampicillin resistance gene, allows selection in *E. coli* (50-100 µg/mL ampicillin); pBS: pBluescript origin of replication, allows propagation of plasmid in *E. coli* at high copy numbers.

2.4 Cloning

2.4.1 Polymerase chain reactions (PCR)

Standard PCR

The components and the temperature program of a standard PCR (e.g. for sub-cloning) can be found in Table 2 and Table 3, respectively. The total volume of the PCR mixtures was 50 µL.

Table 2: Standard PCR-mixture

Component	[μL]
5x Phusion HF Buffer	10.0
dNTP (10 mM)	1.0
forward primer (10 pmol/ μ l)	2.5
reverse primer (10 pmol/ μ l)	2.5
template DNA (plasmid or linear fragment)	1.0
Phusion™ Polymerase (2 U/ μ l)	0.5
ddH ₂ O	32.5

Table 3: Standard PCR-program

Temperature [$^{\circ}$C]	Time	
98	10 sec	
98	15 sec	
65	20 sec	30 cycles
72	< 2 kb: 1 min 30 s > 2 kb: 30 s per kb	
72	10 min	
4	∞	

Overlap extension PCR (OE-PCR)

The reaction mixture in OE-PCRs was the same as in standard PCRs with the exception of using the two fragments to be assembled as the template. The length of the overlapping regions of the two fragments was at least 20 bp and was chosen to match a melting temperature of 65°C (calculated by the Simple Primer Tool OligoAnalyzer 3.1). 10-16 ng of the larger fragment were applied and the other fragment was added in equimolar amounts. The first 8 PCR cycles were performed without primers. Then 2 μ L of each primer solution were added. The temperature program of the second step was the same as for the first one, but the number of cycles was between 22 and 30.

Gibson Assembly

For the Gibson assembly reaction the Gibson Assembly® Cloning Kit (New England Biolabs, Frankfurt, Germany) [47] was used. The assembly reaction was accomplished with 1 µl linear p427TEF without *CYC1_T* (125 ng), 2.2 µL insert DNA – *XUT1_CYC1_T_PdiI* (47 ng), 1.8 µl ddH₂O and 15 µl Gibson Assembly Mastermix 2x. The assembly took place at 50°C for 1 hour.

Colony PCR

Single *E. coli* colonies were resuspended in 50 µL ddH₂O by vortexing. The suspension was heated at 95°C for 5 minutes, followed by centrifugation at 13,200 rpm and 4°C for 1 minute. The colonies of *S. cerevisiae* strains were resuspended in 20 µL of 20 mM NaOH, each. The suspensions were heated at 95°C for 45 min and centrifuged at 13,200 rpm and 4°C for 10 minutes. 2-5 µl of the supernatants of the disrupted *E. coli* or *S. cerevisiae* colonies were used as templates for the PCR. The components and temperature program for colony PCR are shown in Table 4 and Table 5, respectively. Existence of the PCR products was checked by agarose gel electrophoresis (1.5% agarose gel, 1x TAE buffer, 80 V, 90 minutes)

Table 4: PCR-mixture for colony PCR

Component	[µL]
10x Dream Taq Buffer	5
dNTP (10 mM)	1
forward primer (10 pmol/µl)	2
reverse primer (10 pmol/µl)	2
template DNA	3
DreamTaq Polymerase (5 U/µL)	0.5
ddH ₂ O	36.5

Table 5: PCR-program for colony PCR

Temperature [°C]	Time
95	2 min
95	20 sec
65	30 sec
72	< 2 kb: 1 min 30 s > 2 kb: 30 s per kb
72	10 min
4	∞

Primers

Primers used in this study are listed in Table 6.

Table 6: Primer sequences. Grey marked regions show the restriction sites; orange marked letters show the overlapping regions of the *XUT1* gene and *CYC1_T*. Green marked letters show the overlapping region of p427TEF with the *XUT1* gene or the *CYC1_T*.

Nr.	Name	Sequence (5'→3')	Length/bp
1	fw_ <i>NdeI</i> _TEF _p	CTAGGTCATATGCATAGCTTCAAATGTTTCTACTCC TTTTTACTCTCCAGATTTTCTCGGACTC	67
2	rv_ <i>Bsi</i> WI_ <i>CYC1_T</i> -short	CTAGGTCGTACGGTACCGGCCGCAAATTAAGCCTT CG	38
3	fw_Gal2_Pos.85	CCCATTTAAGCGCACAATCTC	21
4	fw_Gal2_Pos.700	GCTATTCGAACTCAGTTCAATGGAGAG	27
5	fw_ <i>Bam</i> HI_ <i>Xut1</i>	CTACTATTGGATCCATGCACGGTGGTGG	28
6	fw_Gal2_ <i>Xma</i> I	CTAGGACCCGGGATGGCAGTTGAGGAGAACAATAT GCCTGTTGTTTC	47
7	rv_Gal2_ <i>Strep</i> -Tag_ <i>Eco</i> RI	CTAGGTGAATTCATTATTTCTCGAACTGAGGATGTGA CCAAGCTGATTCTAGCATGGCCTTGTACCACGG	69
8	rv_ <i>Xma</i> I_ <i>Xut1</i>	GCGTGGTTTCCCGGGTTATTTTCAACGTG	30
9	fw_Insert- <i>Bam</i> HI_ <i>Xut1</i> _long	TAGAACTAGTGGATCCATGCACGGTGGTGGTGACG GTAACGA	42
10	rv_Insert- <i>Xma</i> I_ <i>Xut1</i> _CYC1 _T _long	TCGAATTCCTGCAGCCCGGGTTATTTTCAACGTGG TAGACATCAGCCTTGCTG	54
11	fw_p427TEF_endCYC1 _T _PdII	CACGTTCCGGGCTTCCCGTCAAGCTCTAAA	33
12	rv_p427TEF_beginXut1_ <i>Bam</i> HI	CCACCGTGCATGGATCCACTAGTTCTA	27
13	fw_overlap <i>Xma</i> I_ <i>CYC1_T</i>	AAAATAACCCGGGCTGCAGGAATTCGA	27
14	rv_ <i>CYC1_T</i> _PdII	TTTAGAGCTTGACGGGGAAAGCCGGCGAACGTG	33

Purification of PCR products

The purification of PCR products was done by either using the GeneJET™ PCR-purification Kit, or by running an agarose gel electrophoresis (1.5% agarose gel, 1x TAE buffer, 80 V, 1 h 20 minutes) and subsequent extraction of the respective DNA fragments from the gel, using the GeneJET™ Gel

Extraction Kit. While the purifications were performed according to the manufacturer’s manual, the amounts of sterile ddH₂O for elution of the products were varied between 20 and 50 µL, according to the desired end volume.

2.4.2 Restriction digest and dephosphorylation of vector DNA

Digestion with restriction enzymes was performed sequentially in a total volume of 50 µL at 37°C for 8-16 hours, using the corresponding buffer system, as recommended by the supplier. After digestion of vector DNA with the first restriction enzyme, subsequent dephosphorylation was done for 1 hour at 37°C by adding 2.5 µL fast alkaline phosphatase (Fast AP, 1 U/µL). The phosphatase was removed via the GeneJET™ PCR-purification Kit and the digestion with the second restriction enzyme was started. A list of the used restriction enzymes and their recognition sites can be found in Table 7. After completed restriction digest, the products were purified on an agarose gel (1.5%) and purified by using the GeneJET™ Gel Extraction Kit.

Table 7: Restriction enzymes used and their recognition sites

Enzyme	Recognition site
<i>Bam</i> HI	5'-G↓GATCC-3'
<i>Eco</i> RI	5'-G↓AATTC-3'
<i>Xma</i> I (<i>Cfr</i> 9I)	5'-C↓CCGGG-3'

2.4.3 Ligation of DNA fragments

For ligations of inserts into a dephosphorylated vector, molar ratios of 3:1 to 5:1 of insert to vector were used (Equation 1). Ligation was done with 1 µL T4 DNA ligase (5 U/µL) and 2 µL 10x Ligation Buffer in a total volume of 20 µL either at 16°C over night or at 22°C for 2h.

Equation 1: Calculation of the amount of insert DNA necessary for ligation into a certain vector

$$m_{\text{insert}} = \frac{\text{length}_{\text{insert}} * m_{\text{vector}} * \text{molar ratio}_{\text{insert:vector}}}{\text{length}_{\text{vector}}}$$

m = mass [ng]

length: length [bp]

2.4.4 Transformation (and isolation) of plasmid DNA

***E. coli* transformation**

Transformation of plasmid DNA into *E. coli* cells was done by electroporation. 100 μ L electrocompetent cells were thawed and incubated with either 3 μ L ligation mixture or 1 μ L plasmid preparation on ice for approximately 3 to 5 minutes. Afterwards, cells were electroshocked using the Bs2 setting of a Micro Pulser™ (Bio-Rad, Vienna, Austria) and regenerated in 1 mL SOC medium at 37°C and 500 rpm for 60 min. Cells were plated on LB plates containing the appropriate antibiotic and incubated overnight at 37°C.

For the amplification and isolation of plasmid DNA from *E. coli*, a single colony was picked with a sterile toothpick from an LB-agar plate and inoculated into 5 mL LB medium, supplemented with the required antibiotic, and incubated overnight at 37°C (110 rpm). Cells were harvested by centrifugation (5000 rpm at room temperature for 10 minutes) and the pellet was subjected to plasmid isolation using the GeneJET™ Plasmid Miniprep Kit according to the manufacturer's manual. The DNA was eluted with 50 μ L ddH₂O.

High efficiency transformation of *S. cerevisiae* cells

Expression plasmids were transformed into *S. cerevisiae* strains using a lithium acetate method [48], which was slightly modified. Precultures were either inoculated from YPD plates and grown overnight to an OD₆₀₀ of 10 - 11 or from SDD plates and grown overnight to an OD₆₀₀ of 2.5 - 5. The main cultures were inoculated from the respective precultures to an optical density of 0.2. At an optical density of 0.7-1, cells were harvested via centrifugation (5,000 rpm and room temperature for 5 minutes). Several washing (and concentration) steps were performed as it is described in the protocol [48]. Cell aliquots of 50 μ L were mixed with the reaction solution. The composition of the reaction solution is listed in Table 8. After incubation at 42°C for 40 min the cells were harvested (5,000 rpm, and 4°C for 30 seconds) and the supernatant was discarded. Cells were gently resuspended in 500 μ L YPD medium and regenerated for at least 3 hours at 30°C and 300 rpm on a thermomixer. Appropriate dilutions of the cell suspension were plated on selection medium after regeneration and incubated at 30°C for 2 to 3 days.

Table 8: Reaction mixture for lithium acetate method

Reaction solution	[μ L]
PEG 3640 50% (w/v)	240
Lithium acetate 1 M	36
Boiled SS-carrier DNA [2 mg/mL]	50
Plasmid DNA plus sterile ddH ₂ O	34
Total	360

Zymolyase-treatment and subsequent plasmid DNA purification

For the amplification and isolation of plasmid DNA from *S. cerevisiae*, several single colonies were picked with sterile toothpicks from agar plates and grown in 50 mL selection media, each. Cells were harvested, washed with 0.9% sodium chloride and plasmid DNA was isolated by using Lysis buffer (5mg/mL zymolyase 20T, 1M sorbitol, 50 mM EDTA, 100 mM PPB buffer, 20 μ L RNase solution) together with the bacterial GeneJET™ Plasmid Miniprep Kit from Thermo Scientific (starting with step number 2). The DNA was eluted with 50 μ L ddH₂O.

2.5 Construction of yeast reference strains and strains, expressing the Gal2_N376F or XUT1 transporter.

2.5.1 Construction of the reference strains *S. c.* XR (g)-p427TEF, *S. c.* XR (2 μ)-p427TEF and *S. c.* IBB10B05-p427TEF

The empty plasmid p427TEF was amplified in *E. coli* TOP 10 cells and subsequently transformed into *S. c.* XR (2 μ) and *S. c.* IBB10B05 to obtain the reference strains *S. c.* XR (2 μ)-p427TEF and *S. c.* IBB10B05-p427TEF, respectively.

2.5.2 Construction of strains, expressing the Gal2_N376F transporter

The plasmid p427TEF was amplified in *E. coli* TOP10 cells and digested with the restriction enzymes *Xma*I and *Eco*RI. The pUC57-Kan plasmid, carrying the *GAL2_N376F* transporter gene, was also amplified in *E. coli* TOP10 cells and digested with *Xma*I and *Eco*RI. The resulting *GAL2_N376F* gene was ligated into the multiple cloning site of the prepared p427TEF vector, just between the TEF1

promoter and the $CYC1_T$ sequences. The p427TEF-Gal2_N376F expression plasmid was transformed into *S. c.* XR (g), *S. c.* XR (2 μ) and *S. c.* IBB10B05 to yield the strains *S. c.* XR (g)-Gal2M, *S. c.* XR (2 μ)-Gal2M and *S. c.* IBB10B05-Gal2M, respectively.

Construction of a strain expressing Gal2_N376F transporter tagged with a Strep-TagII

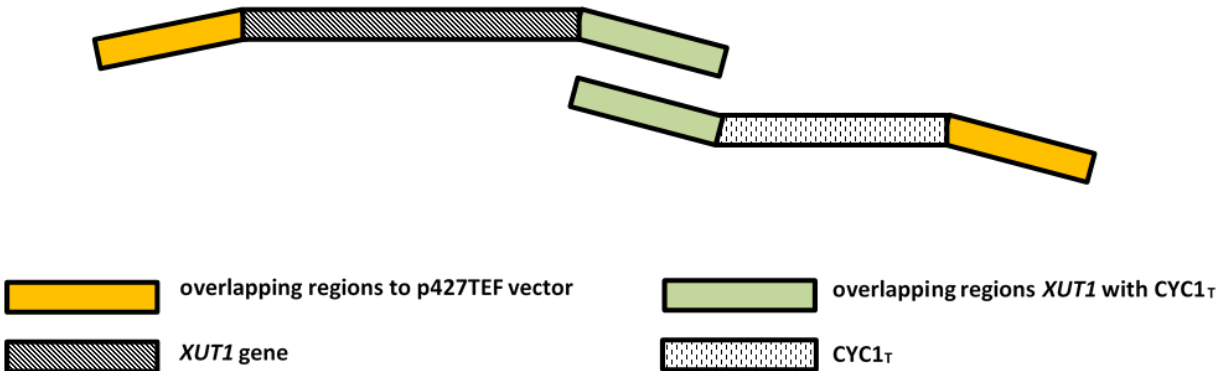
For the construction of the *S. c.* XR (2 μ)-Gal2M-Strep strain, a Strep-TagII sequence was C-terminally attached to the *GAL2_N376F* gene by using the primers 6 and 7 (Table 6) for PCR and pUC57-Kan plasmid as the template. *XmaI* and *EcoRI* restriction sites were added via the same PCR. Further cloning steps were performed as it is described for the preparation of the p427TEF-Gal2_N376F plasmid to yield the plasmid p427TEF-Gal2_N376F-Strep. The vector was transformed into *S. c.* XR (g), *S. c.* XR (2 μ) and *S. c.* IBB10B05 to yield the strain *S. c.* XR (g)-Gal2M-Strep, *S. c.* XR (2 μ)-Gal2M-Strep and *S. c.* IBB10B05-Gal2M-Strep, respectively.

2.5.3 Construction of strains, expressing the XUT1 transporter

A schematic overview of the cloning strategy for the construction of the p427TEF vector carrying the *XUT1* transporter gene can be found in Figure 2. The expression plasmid was assembled using overlap extension PCR and Gibson Assembly. In a first step the p427TEF vector was amplified in *E. coli* TOP10 cells. The obtained plasmid was used for generation of the p427TEF vector backbone fragment without $CYC1_T$. Therefore the primers 11 and 12 (Table 6) were used. The second fragment that was needed was the $CYC1_T$ fragment including overlapping regions to the *XUT1* gene and the p427TEF backbone. This fragment was generated by using the primers 13 and 14 for PCR and p427TEF plasmid as the template.

The pEX-K4 plasmid, carrying the *XUT1* transporter gene, was amplified in *E. coli* DH5 α cells at room temperature, to prevent a toxic effect of the foreign gene on the *E. coli* cells. The plasmid was used for PCR to amplify the *XUT1* gene with overlapping regions to the TEF promoter of p427TEF vector and the $CYC1_T$ (primers 9 and 10). Assembling of the *XUT1* fragment and the $CYC1_T$ fragment was done by using OE-PCR. Gibson cloning was chosen to be suitable for assembling the p427TEF vector backbone fragment without $CYC1_T$ and the generated *XUT1*- $CYC1_T$ fragment. The resulting plasmid, p427TEF-Xut1, carries the *XUT1* gene located between the TEF1 promoter and the $CYC1_T$. The plasmid was transformed into *S. c.* XR (2 μ) and *S. c.* IBB10B05 to yield the strains *S. c.* XR (2 μ)-Xut1 and *S. c.* IBB10B05-Xut1.

Step 1: assembling of *XUT1* with *CYC1 τ*



Step 2: assembling of p427TEF vector backbone with the *XUT1*-*CYC1 τ* fragment

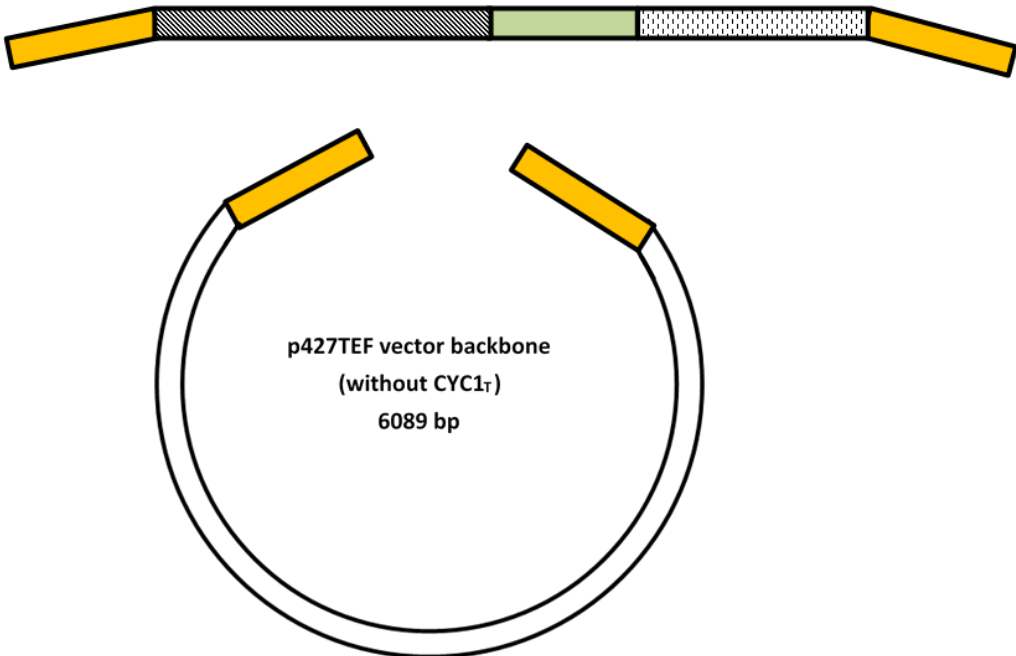


Figure 2: Schematic overview of the construction of the p427TEF vector carrying the *XUT1* gene.

2.6 Xylose fermentations

2.6.1 (Semi-)aerobic fermentations in shaking flasks

Cultivation of strains and production of biocatalyst biomass

All xylytol-producing yeast strains were cultivated at 30°C in baffled shaking flasks (300 mL flasks containing 50 mL of preculture or 1000 mL flasks containing 300 mL of main culture) using an agitation rate of 120 rpm. *S. c.* XR(g)-p427TEF, *S. c.* XR(g)-Gal2M and *S. c.* XR(g)-Xut1 were grown in YPD medium with Geneticin-Sulfat (G418). *S. c.* XR(g) was grown solely in YPD medium. The strains *S. c.* XR (2μ)-p427TEF, *S. c.* XR (2μ)-Gal2M, *S. c.* XR (2μ)-Xut1 were grown in SDD medium containing G418 as the selective marker. The strain *S. c.* XR (2μ) was grown solely in SDD medium.

Precultures were either inoculated from YPD-G418 plates and grown over night to an OD₆₀₀ of 10 - 11 or from SDD-G418 plates and grown over night to an OD₆₀₀ of 2.5 - 5. The main cultures were inoculated from the respective precultures to an optical density of 0.05. At an optical density of ~ 5, the biomass of the main cultures was harvested by centrifugation at 5,000 rpm and 4°C for 20 minutes. The supernatants were removed and the pellets were resuspended in 20 mL 0.9% sterile sodium chloride and transferred into a 50 mL Sarsted tube, followed by another centrifugation step (vide supra). After removing the supernatants, the pellets were resuspended in the respective media to yield a total volume of 20 mL suspension. The optical densities of the cell stocks were determined in order to assess the volumes that were required to inoculate media for the batch conversions.

Batch conversion and sample preparation

Batch conversions were performed in 300 mL baffled shaking flasks containing a final volume of 50 mL, consisting of the respective medium, the biocatalyst (starting OD₆₀₀ 1-5), 15 g/L xylose as the substrate and ~27 g/L glucose or ~ 9.2 g/L ethanol as the co-substrate. Bio-conversions were shaken at 120 rpm at 30°C over a time period of at least 24 hours. Samples (1040 μL each), were taken regularly and the optical densities were determined spectrophotometrically. The remaining 940 μL of each sample were centrifuged at 13,200 rpm and 4°C for 10 minutes. The supernatants were transferred to an HPLC vial and stored at -20°C.

2.6.2 Anaerobic fermentations

Cultivation of strains and production of biocatalyst biomass

All precultures of the ethanol-producing yeast strains were cultivated aerobically at 30°C in baffled shaking flasks (300 mL flasks containing 50 mL of preculture) using an agitation rate of 120 rpm. The parental strain *S. c.* IBB10B05 was grown in M- medium containing 20 g/L glucose, the strains *S. c.* IBB10B05-Gal2M and *S. c.* IBB10B05-Xut1 were grown in M- medium containing 20 g/L glucose and G418. Main cultures were inoculated from the respective precultures to an optical density of 0.05-0.1. Cells were grown anaerobically in sealed flasks (100 mL airproof flasks containing 90 mL main culture) at 30°C for three days using an agitation rate of 200 rpm. The main culture medium consisted of M- medium containing 20 g/L xylose with or without G418. The main cultures were harvested (vide supra) and used for the anaerobic batch conversion experiments.

Batch conversion and sample preparation

Anaerobic batch conversions were performed at 30°C and 200 rpm in M- medium using 100 mL airproof flasks containing a final volume of 90 mL. 50 g/L xylose were used as the substrate. Over a time period of 96 hours, samples (2 mL each), were taken and the optical density was determined spectrophotometrically. The remaining 1 mL of the sample was centrifuged at 13,200 rpm and 4°C for 10 minutes. The supernatant was transferred to an HPLC vial and stored at -20°C.

2.7 Analytical methods

2.7.1 Protein analytics

Preparation of protein extracts

Protein extracts of different yeast strains were prepared by a TCA precipitation protocol derived from Rietzmann [49], which was slightly modified. 10 OD₆₀₀ units of cells were transferred to Eppendorf tubes, mixed with Y-Per (Thermo Scientific – Life Technologies, St. Louis, USA) reagent and shaken at 300 rpm and 22°C for 20 minutes. After centrifugation (12,000 rpm and 4°C for 10 minutes) cell pellets were resuspended in 300 µL of 1.85 M NaOH and 7.5 (v/w) β-mercaptoethanol and kept on ice for 1 hour. 300 µL of 50% TCA were added to the mix, vortexed rigorously and left on ice for 2 hours. Cell lysate fractions were treated only with 50% TCA (end-concentration of TCA was 25%). The samples were centrifuged at 13,200 rpm and 4°C for 10 minutes and the supernatant was discarded. The pellets were each resuspended in 100-150 µL of a mix containing 25 µL NuPAGE

sample buffer (4x), 10 μ L NuPAGE reducing agent DTT (10x), and 65 μ L ddH₂O. Dissolving the pellet of the lysate fraction was only possible by using an ultrasonic bath for 5 min. Samples for SDS-PAGE were denatured at 95°C for 5 min.

SDS Page

The NuPage® electrophoresis system from Thermo Scientific with 4-12% BisTris gels was used. The gels were run in MOPS-Buffer for at least 50 minutes with the specifications of the NuPage Gel program (a maximum of 200 V, 120 mA and 25 W) and stained with Coomassie staining solution.

Western Blot

Following TCA precipitation, proteins were separated via SDS-PAGE and blotted to a nitrocellulose membrane by following the NuPage protocol for electrophoresis and Western blotting. The blotting sandwich was prepared as shown in Figure 3. Protein transfer was performed in 1x Tris Glycine Transfer Buffer at a current of 200 mA for 60 min.

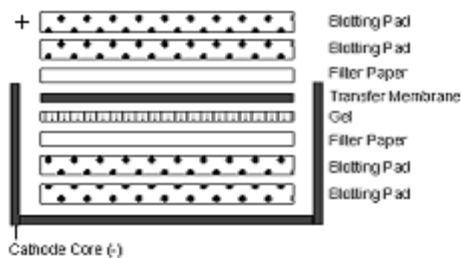


Figure 3: Scheme for Western Blot assembly, (copyright by Invitrogen)

To check if the transfer was successful, the membrane was stained with PonceauS. An image was taken and the membrane was destained with 1x PBS. Blocking of the membrane was carried out overnight at 4°C in 20 mL blocking solution. Strep-tagged proteins were detected using the Strep Tag II monoclonal antibody (AB) (1:10,000 in 20 mL of PBST) as first AB and HRP-conjugated goat anti-mouse AB (1:10 000 in 40 mL of PBST/2.5% BSA) as secondary AB. The primary AB was incubated at 4°C overnight and the secondary AB was incubated 1 hour at room temperature while shaking moderately. Between the two steps and before detection, the membrane was washed three times, each 5 minutes, with PBST. The substrate for signal generation was from the Thermo Scientific Chemiluminescence Super Signal® West Pico Kit and it was applied as written in the manual. The chemoluminescence signal was detected by exposure to a photographic film for 3 to 5 minutes.

2.7.2 Determination of XR activity in cell free extracts

Yeast cell disruption

For the determination of protein concentration and enzyme activity 50-60 OD₆₀₀ units of cells (harvested and washed main culture) were used. The disruption mix contained pelleted cells, glass beads (1 w/w) and 100 mM PPB (2 v/w). Cells were disrupted by 10 cycles of rigorously mixing the disruption suspension for 30 seconds and keeping the cells on ice for 30 seconds between these steps. To get the crude cell extract, the disruption suspension was subsequently centrifuged at 13,200 rpm and 4°C for 10 minutes.

Determination of protein concentration

The protein concentration in the crude cell extracts was determined based on the method of Bradford, using the Roti-Quant protein quantification assay according to the manufacturer's procedure. Samples were diluted 1:20, 1:40 and 1:80 in 100 mM PPB. A BSA calibration curve (0-1 mg/mL) served as the protein standard for quantification.

Determination of XR activity

XR activity was assayed spectrophotometrically at 340 nm by monitoring the oxidation of NAD(P)H for 10 minutes. One unit of enzyme activity refers to 1 μmol of NAD(P)H consumed per minute. All activity measurements were performed with a Beckman DU-800 spectrophotometer thermostated at 25°C. Reactions were carried out in 100 mM PPB, supplemented with xylose (final concentration of 700 mM) and started either by the addition of NAD(P)H (final concentration of 0.3 mM) or by the addition of the crude cell extract. Reactions without substrate and without enzyme served as negative controls. Therefore, 100 mM PPB was used instead of xylose or the crude cell extract.

2.7.3 Analysis of fermentation products (HPLC measurements)

HPLC-analysis of the metabolites glucose, xylose, xylitol, glycerol, acetate and ethanol was performed on a LaChrom HPLC system (Merck) or a Shimadzu HPLC system (for detailed apparatus information see appendix chapter 6.3), both equipped with an RI detector and a thermostated column oven. Samples were analyzed on an Aminex HPX-87H column (Bio Rad Laboratories, Vienna, Austria) using 5 mM sulphuric acid as eluent at a flow rate of 0.6 mL/min and a temperature of 65°C. Peaks were identified and quantified based on authentic standards with known concentrations.

2.7.4 Determination of growth rates

For the determination of specific growth rates (μ), a linear regression from the linear part of the logarithmic plotting of OD₆₀₀ values versus time was done. Average values and deviations of double determinations are shown.

2.7.5 Determination of yields

Yields ($Y_{\text{xylitol}} [g_{\text{Xol}}/g_{\text{Xyl}}]$) of xylitol producing strains were defined as the total amount of produced xylitol divided by the total amount of xylose added to the reaction (not xylose consumed by the cells), whereby losses due to sampling were considered. Yields ($Y_{\text{ethanol}} [g_{\text{EtOH}}/g_{\text{Xyl}}]$) of ethanol producing strains were defined as the total amount of produced ethanol divided by the total amount of xylose added to the reaction. Co-substrate yields for glucose and ethanol ($g_{\text{Xol}}/g_{\text{Glc}}$ or $g_{\text{Xol}}/g_{\text{EtOH}}$) were determined similarly: the total amount of produced xylitol was divided by the total amount of co-substrate (glucose or ethanol) added to the reaction [50]. Calculated values represent the xylitol yields and co-substrate yields after 24 h and ethanol yields after 96 h. Average values and deviations of double determinations are shown.

2.7.6 Determination of xylose uptake rates and xylitol or ethanol productivities

To study the xylose uptake and product formation the xylose decrease and xylitol or ethanol production was monitored. For the calculation of the volumetric xylose uptake rates and xylitol or ethanol productivities the determined xylose, xylitol or ethanol values were plotted versus time. The slope of the linear regression from the linear part of the plotting (volumetric rates) and the cell dry weight (CDW) of the cells were set in correlation to get the maximal specific xylose uptake rates and maximal specific xylitol and ethanol productivities.

3 Results and Discussion

In order to characterize xylose uptake profiles in the presence of additional transporters, two genes were recombinantly expressed in *S. cerevisiae*. The transporters Gal2_N376F and Xut1 were selected based on literature evidence of xylose transport capacity [17, 25]. A total of five *S. cerevisiae* strains expressing either Gal2_N376 or the Xut1 transporter were constructed and investigated in regard to their xylose uptake and xylitol or ethanol production rates.

3.1 *E. coli* subcloning and *S. cerevisiae* transformation

A detailed description of the cloning strategy can be found in Material and Methods (section 2.4 and 2.5.). The construction of expression plasmids using a standard cloning procedure (PCR, restriction digest, ligation, transformation) and *E. coli* TOP10 cells was successful for the *GAL2_N376F* gene and the construct with the C-terminally attached Strep-Tag sequence (Gal2_N376F-Strep). The presence of p427TEF-Gal2_N376F and p427TEF-Gal2_N376F-Strep expression plasmids was verified by colony PCR and agarose gel electrophoresis (section 2.4.1). Sequencing (LGC genomics GmbH) was used for confirming sequence correctness and absence of mutations in the genes.

The expression plasmids p427TEF-Gal2_N376F and p427TEF-Gal2_N376F-Strep were transformed into *S. c.* XR (g), *S. c.* XR (2 μ) and *S. c.* IBB10B05. The empty plasmid p427TEF was transformed into *S. c.* XR (2 μ) and *S. c.* IBB10B05. The presence of the respective plasmids in the different yeast strains was verified via colony PCR using forward primer 1 and reverse primer 2 (Table 6). PCRs from clones harboring the Gal2_N376F transporter yielded a DNA-fragment with a length of ~2.5 kilo base pairs (kbp). p427TEF-Gal2_N376F served as a positive control and as negative control the empty plasmid p427TEF, yielding a 0.75 kbp DNA-fragment, was chosen. Examples of agarose gel electrophoresis analyses can be found in Figure 4 and Figure 5.

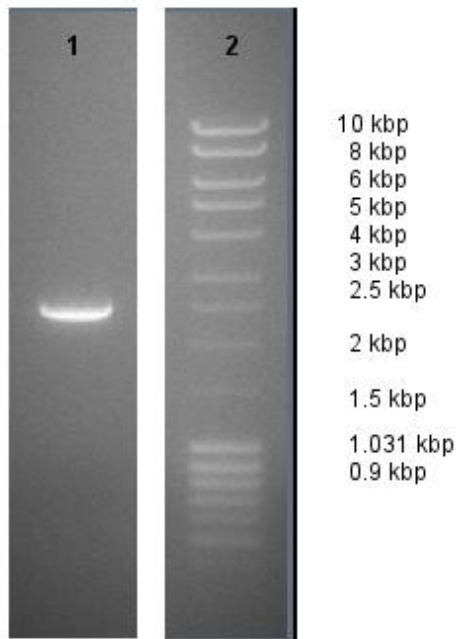


Figure 4: Agarose gel electrophoresis of the colony PCR of *S. c. XR (g)-Gal2M*; Lane 1: The band at 2.5 kbp indicates a positive clone that harbors the *GAL2_N376F* gene. Lane 2: Mass Ruler DNA Ladder Mix.

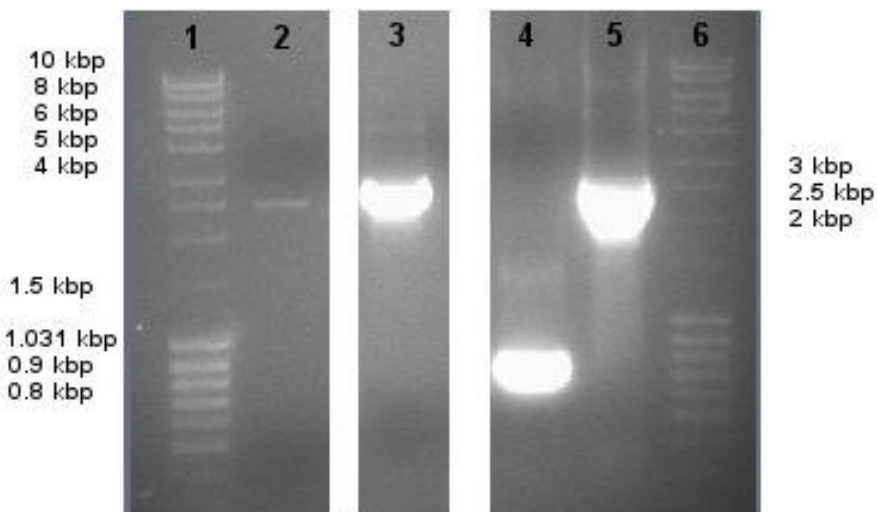


Figure 5: Agarose gel electrophoresis of the colony PCR of *S. c. IBB10B05-Gal2M*. Lane 1 and 6: Mass Ruler DNA Ladder Mix. Lane 2 and 3: Bands at 2.5 kbp indicate positive clones that harbor the *GAL2_N376F* gene. Lane 4: Negative control (p427TEF plasmid). Lane 5: Positive control (p427TEF-Gal2_N376F plasmid).

The cloning strategy for the Xut1 transporter differed from the standard cloning procedure due to issues with several common cloning steps. The PCR from the original plasmid that carried the *XUT1* transporter gene pEX-K4-XUT1 gave low yields and was not reproducible. *E. coli* Top10 cells, that were transformed with the pEX-K4-XUT1 vector, showed impaired growth, low plasmid yields and the restriction digest pattern of the isolated plasmid was ambiguous. These problems led to the assumption that the existence of the *XUT1* gene from *P. stipitis* in the shuttle plasmid had toxic effects on the used *E. coli* cells. To overcome the problems of isolating and amplifying the *XUT1* gene, the cloning strategy was switched to Gibson assembly (section 2.5.3) and the host strain was changed to *E. coli* DH5 α . Additionally, bacterial growth temperature was set to room temperature instead of 37 °C, which finally led to positive transformants. Once cloned into the shuttle vector p427TEF, the absence of mutations in the *XUT1* gene was confirmed by sequencing. The sequences of the transporters can be found in the Appendix.

The expression plasmid p427TEF-Xut1 was transformed into *S. c.* XR (2 μ) and *S. c.* IBB10B05. The presence of the plasmid in the *S. cerevisiae* strains could not be verified via colony PCR. Therefore, plasmids of several clones were isolated (Zymolyase-treatment and subsequent plasmid DNA purification KIT from Thermo Scientific) and control PCRs with the primers 9 and 10 (Table 6) were performed, resulting in ~1.7 kbp DNA fragments for positive clones (see Figure 6). The corresponding sequenced plasmid served as a positive control and as negative control the empty plasmid p427TEF was taken. The negative control did not show a band, because the reverse primer could not find a complementary sequence when the *XUT1* gene was not present.

A list of all constructed and parental strains used for this study can be found in Table 9.

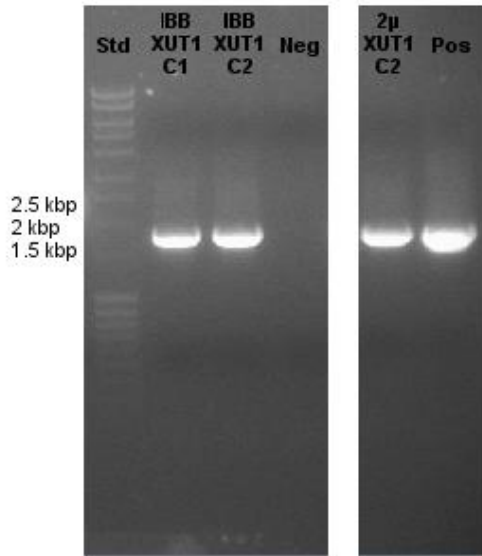


Figure 6: Agarose gel electrophoresis of the control PCR of *S. c. XR (2 μ)-Xut1* and *S. c. IBB10B05-Xut1*; Std: Mass Ruler DNA Ladder Mix. IBB XUT1 C1 and C2: *S. c. IBB10B05-Xut1* clone number 1 and 2, the bands at ~ 1.7 kbp indicate positive clones that harbor the *XUT1* gene. Neg: negative control p427TEF. 2 μ XUT1 C2: *S. c. XR (2 μ)-Xut1* clone number 2, the band at ~ 1.7 kbp indicates a positive clone. Pos: positive control p427TEF-Xut1.

3.2 XR activities in recombinant *S. cerevisiae* strains

Intracellular XR activity is a crucial factor in microbial xylose utilization. Therefore, we have compared the XR activities of four engineered *S. cerevisiae* strains and their parental strains in order to determine whether the presence of the additional xylose transporters alters the reductase's expression level. Since the *CtXR* gene has been shown to have a natural preference for NADPH over NADH [22], all activity measurements were performed with NADPH as the co-enzyme. The protein concentrations in the crude cell extracts of the strains were determined and used to calculate the specific XR activities (U/mg_{Prot}). Mean values are summarized in Table 9.

No difference in the XR activities was observable when comparing *S. c. XR (g)* (0.08 ± 0.01 U/mg_{Prot}) and *S. c. XR (g)-Gal2M* (0.09 U/mg_{Prot}), which reveals that the presence of the p427TEF multi copy plasmid, carrying the transporter sequence, did not affect the XR activity of the strain that harbored the *CtXR* expression cassette in the genome. Intracellular XR activities were much higher in the strains that carried multiple copies of the yeast 2 μ expression vector p426GPD-XR. *S. c. XR (2 μ)* showed an

XR activity of 0.86 ± 0.04 U/mg_{Prot}, which is 10-fold higher than the activity of the *S. c.* XR (g) strain. The *S. c.* XR (2 μ)-p427TEF strain that carried the empty expression vector had nearly the same XR activity (0.82 ± 0.03 U/mg_{Prot}), although this strain held two different multiple copy plasmids. This observation indicates that the presence of the additional expression vector p427TEF had no influence on the XR activity of the yeast strain. However, the expression of a transporter gene using the p427TEF plasmid decreased the XR activity of the strain. 1.3-fold and 1.2 fold lower XR activities were obtained with the strains *S. c.* XR (2 μ)-Gal2M (0.65 ± 0.03 U/mg_{Prot}) and *S. c.* XR (2 μ)-Xut1 (0.74 ± 0.03 U/mg_{Prot}), respectively, compared to the *S. c.* XR (2 μ). A change in the ratio of protein content, due to the additional overexpression of a transporter protein can probably explain the decrease of the XR activity. Further influencing factors on the expression level of a protein are the strength of the promoter, regulatory elements downstream of the promoter and differences in the copy number of the plasmids. A 15-fold higher XR activity was obtained with the *S. c.* IBB10B05 compared to the *S. c.* XR (g). Both strains harbored the *CtXR* expression cassette in the genome under the control of the TDH3 (formerly GPD) promoter. The difference in the XR activities may result from the evolution steps of the *S. c.* IBB10B05 on xylose as the only substrate, which can bring about an upregulation of the *CtXR* gene expression [21]. XR activity was not determined in the strains *S. c.* IBB10B05-Gal2M and *S. c.* IBB10B05-Xut1.

Table 9: *S. cerevisiae* strains used in this study. Grey marked: parental strains; bold: additionally introduced modification

Strain name	Parental strain	Strain background	Plasmids	Activity (U/mg _{Prot})
<i>S. c.</i> XR (g)	<i>S. c.</i> CEN.PK 113-5D	XR		0.08 ± 0.01
<i>S. c.</i> XR (g)-Gal2M	<i>S. c.</i> CEN.PK 113-5D	XR	p427TEF-Gal2_N376F	0.09 ± 0.01
<i>S. c.</i> XR (g)-Gal2M-Strep	<i>S. c.</i> CEN.PK 113-5D	XR	p427TEF-Gal2_N376F-Strep	n. d.
<i>S. c.</i> XR (2μ)	<i>S. c.</i> CEN.PK 113-5D	XR	p426GPD-XR	0.86 ± 0.04
<i>S. c.</i> XR (2μ)-p427TEF	<i>S. c.</i> CEN.PK 113-5D	XR	p426GPD-XR, p427TEF	0.82 ± 0.03
<i>S. c.</i> XR (2μ)-Gal2M	<i>S. c.</i> CEN.PK 113-5D	XR	p426GPD-XR, p427TEF-Gal2_N376F	0.65 ± 0.03
<i>S. c.</i> XR (2μ)-Gal2M-Strep	<i>S. c.</i> CEN.PK 113-5D	XR	p426GPD-XR, p427TEF-Gal2_N376F-Strep	n. d.
<i>S. c.</i> XR (2μ)-Xut1	<i>S. c.</i> CEN.PK 113-5D	XR	p426GPD-XR, p427TEF-Xut1	0.74 ± 0.03
<i>S. c.</i> IBB10B05	<i>S. c.</i> IBB10B05	XR, XDH, XKS		(a) 1.2 ± 0.03
<i>S. c.</i> IBB10B05-p427TEF	<i>S. c.</i> IBB10B05	XR, XDH, XKS	p427TEF	n. d.
<i>S. c.</i> IBB10B05-Gal2M	<i>S. c.</i> IBB10B05	XR, XDH, XKS	p427TEF-Gal2_N376F	n. d.
<i>S. c.</i> IBB10B05-Gal2M-Strep	<i>S. c.</i> IBB10B05	XR, XDH, XKS	p427TEF-Gal2_N376F-Strep	n. d.
<i>S. c.</i> IBB10B05-Xut1	<i>S. c.</i> IBB10B05	XR, XDH, XKS	p427TEF-Xut1	n. d.

n. d. not determined; (a) value from literature [21]

3.3 The effect of xylose transporter expression in a xylitol-producing low-XR-activity strain

To study the xylose uptake and product formation in a xylitol-producing low-XR-activity strain *S. c.* XR (g) and *S. c.* XR (g)-Gal2M were monitored during batch conversions of 15 g/L xylose. The determined parameters were cell growth, measured via optical density at 600 nm, and the metabolite concentrations of glucose, xylose, xylitol, glycerol and ethanol by using HPLC analysis. The results are shown in Figure 7. Using data of the end point analyses after 120 hours, the xylitol and co-substrate yields of the different strains were calculated and summarized in Table 10. Initial xylose uptake rates (0-3 hours) and initial xylitol productivities did not exceed 0.08 g_{xyI}/(L*h) and 0.01 g_{xyI}/(L*h), respectively. Therefore, data acquired between 4 and 24 hours were used for the determination of the maximal volumetric xylose uptake rates (see Figure 7c). The slope of the volumetric rates and the cell dry weight (CDW) of the cells were set in correlation to get the maximal specific xylose uptake rate and maximal specific xylitol productivity (see Table 10).

A 1.3-fold lower xylitol yield was obtained with the *S. c.* XR (g)-Gal2M strain (0.26 g/g) compared to the *S. c.* XR (g) strain (0.36 g/g). Generally, the xylitol yields achieved with this experimental set up were relatively low, due to a start OD₆₀₀ of 1. The low start OD₆₀₀ was chosen to be able to detect small changes in the xylose uptake profile. This was not possible due to a relatively high deviation of the data during the initial phase. Comparing the volumetric xylose uptake rates, a similar decrease (1.4-fold) was observed when *S. c.* XR (g)-Gal2M strain was used. However, no significant difference in the specific xylose uptake rates was detectable, which indicates that expression of the transporter did neither decrease nor increase cellular xylose uptake rates. The differences in volumetric uptake rates and yields rather stem from the differences in cell proliferation.

Table 10: Sugar uptake rates and yields during xylose reduction by *S. c. XR (g)* and *S. c. XR (g)-Gal2M*.

Parameter	<i>S. c. XR (g)</i>	<i>S. c. XR (g)-Gal2M</i>
Start OD ₆₀₀ /End OD ₆₀₀	0.9/10.6	0.9/9.3
μ [1/h] ^a	0.45	0.37
Y_{xylitol} [g _{Xol} /g _{Xyl}] ^b	0.36	0.26
$Y_{\text{co-substrate}}$ [g _{Xol} /g _{Glc}] ^b	0.22	0.15
Volumetric xylose uptake rate [g _{Xyl} /(L*h)]	0.32	0.22
Specific xylose uptake rate [g _{Xyl} /(g _{CDW} *h)] ^c	0.08	0.07
Volumetric xylitol productivity [g _{Xol} /(L*h)]	0.31	0.22
Specific xylitol productivity [g _{Xol} /(g _{CDW} *h)] ^c	0.08	0.07
Volumetric glucose uptake rate* [g _{Glc} /(L*h)]	1.47	1.36
Specific glucose uptake rate* [g _{Glc} /(g _{CDW} *h)] ^b	2.26	2.20

^aM.D's on μ were $\leq 10\%$. ^bM.D's on yields were $\leq 2\%$. ^cM.D's on specific rates and specific productivities were $\leq 40\%$. *rate determined using data of 0-3 hours;

Due to the use of glucose as the co-substrate, the initial specific glucose uptake rates were also determined. No significant difference in the specific glucose uptake rates of *S. c. XR (g)* (2.26 g_{Glc}/(g_{CDW}*h)) and *S. c. XR (g)-Gal2M* (2.20 g_{Glc}/(g_{CDW}*h)) was detectable. Based on the absent ability of the Gal2_N376F transporter to transport glucose [25], this result seems reasonable. An overexpression of the Gal2_N376F transporter should not influence the glucose uptake rates.

As a result of no detectable difference in sugar uptake performance of the strains lacking and containing the Gal2_N376F transporter, further experiments with other strains and with ethanol as the co-substrate were performed to be able to interpret the data. Furthermore, the parental strain is not totally comparable with a strain that harbors a multi-copy plasmid, regarding the metabolism of the cells. An additional plasmid can result in a metabolic burden on the *S. cerevisiae* strain, followed by a negatively influenced metabolism. To exclude that a possible difference in xylose uptake behavior might have been overlooked, a suitable reference strain harboring the p427TEF plasmid became necessary for comparison.

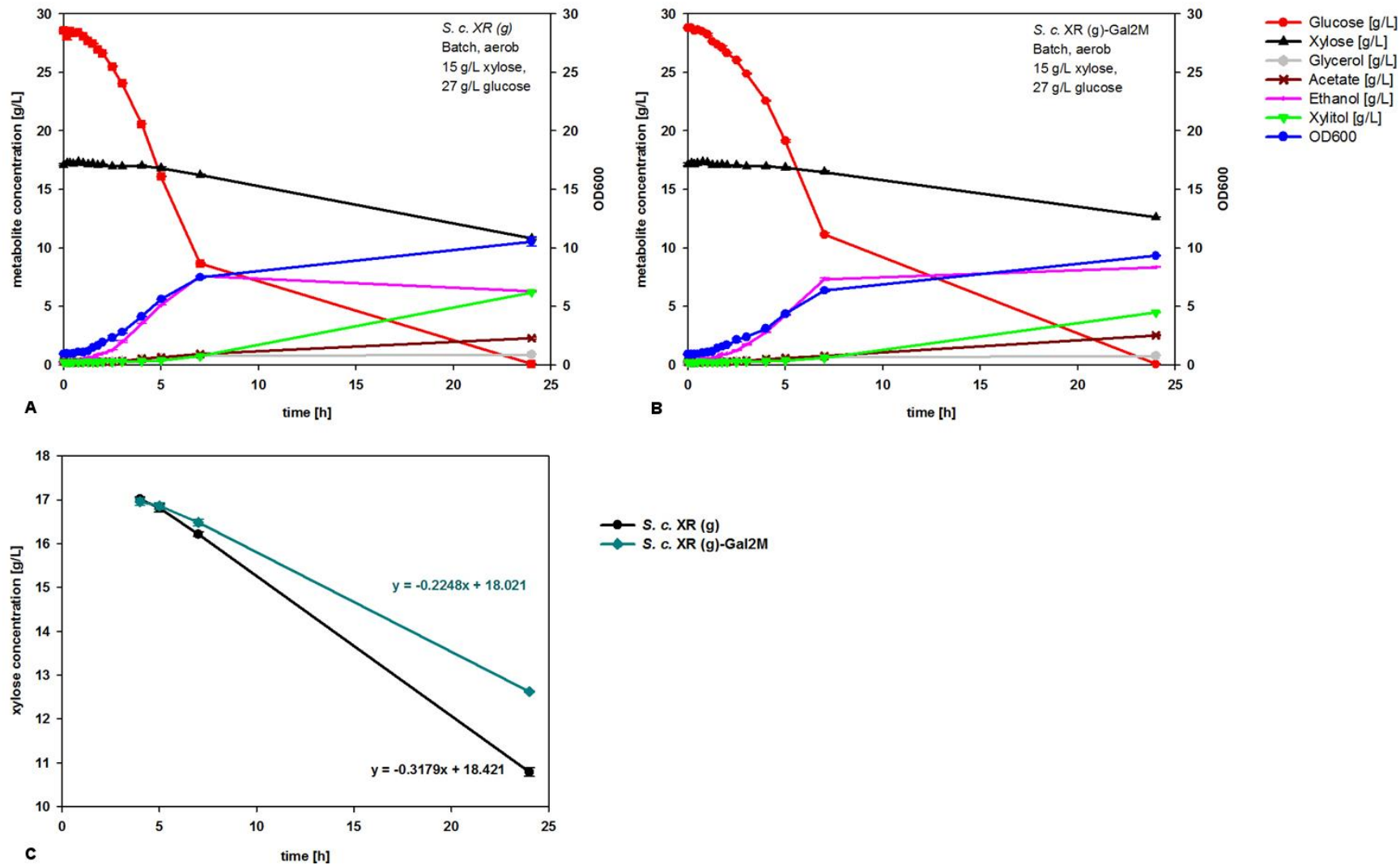


Figure 7: Xylose utilization and product formation during batch conversion in shake flask cultivation of *S. c. XR (g)* [A] and *S. c. XR (g)-Gal2M* [B]. Xylose, xylitol, glycerol, ethanol, acetate and glucose were analyzed by HPLC. Growth was monitored via OD₆₀₀ determination. Initial xylose uptake profiles and slopes of *S. c. XR (g)* and *S. c. XR (g)-Gal2M* are shown in panel C.

3.4 The effect of xylose transporter expression in a xylitol-producing high-XR-activity strain

Co-fermentation of glucose and xylose was tested with the strains *S. c.* XR (2 μ), *S. c.* XR (2 μ)-p427TEF, *S. c.* XR (2 μ)-Gal2M and *S. c.* XR (2 μ)-Xut1. Batch conversions were started in this and following experiments with an OD₆₀₀ of 5. However, *S. c.* XR (2 μ) was not included in the strain comparison due to a too low start OD₆₀₀ (3.0). The time courses of the conversions are displayed in Figure 8. Comparison of the strains *S. c.* XR (2 μ)-p427TEF and *S. c.* XR (2 μ)-Gal2M showed no significant difference in xylitol yields (0.74-0.78 g/g), maximal specific xylose uptake rates (0.08 g_{xyI}/(g_{CDW}*h)) or maximal specific xylitol productivities (0.08 g_{xol}/(g_{CDW}*h)). Using the *S. c.* XR (2 μ)-Xut1 strain a 1.2-fold decrease in xylitol yield (0.65 g/g) was detected (see Table 11). A trend of a less effective xylose uptake behavior of the strain harboring the transporter is visible, when comparing the maximal specific xylose uptake rates of the strains *S. c.* XR (2 μ)-p427TEF (0.08 g_{xol}/(g_{CDW}*h)) and *S. c.* XR (2 μ)-Xut1 (0.04 g_{xol}/(g_{CDW}*h)). The maximal xylose uptake rates and xylitol productivities obtained with *S. c.* XR (2 μ)-p427TEF and *S. c.* XR (2 μ)-Gal2M are the same as those obtained with the *S. c.* XR (g) and *S. c.* XR (g)-Gal2M strains. This observation indicates that specific xylose uptake and xylitol productivity are – under the chosen conditions – not dependent on intracellular XR activity, which in turn suggests that limitations stem from insufficient co-factor supply or recycling and/or xylose transport. Referring to these data, the overexpression of the Gal2_N376F transporter is questionable. Analysis of the overexpression of the Gal2_N376F transporter was performed via Western Blot analysis and the results of the investigation can be found in section 3.6. Additionally, among other factors the expression of the several yeast hexose transporter (*HXT*) genes is strongly regulated by the presence and concentration of glucose [29, 51, 52]. Therefore, the assumption of a masking effect by automated upregulation of native hexose transporter expression should be taken into account.

Initial specific glucose uptake rates were also determined. A decrease of the initial glucose uptake rate (1.35-fold) was detectable when comparing *S. c.* XR (2 μ)-p427TEF (1.84 g_{GlC}/(g_{CDW}*h)) and *S. c.* XR (2 μ)-Xut (1.36 g_{GlC}/(g_{CDW}*h)). The initial glucose uptake rate of the *S. c.* XR (2 μ)-Gal2M was the lowest rate (1.13 g_{GlC}/(g_{CDW}*h)) compared to the other two strains.

Table 11: Sugar uptake rates and yields during xylose reduction by *S. c.* XR (2 μ), *S. c.* XR (2 μ)-Gal2M, *S. c.* XR (2 μ)-p427TEF and *S. c.* XR (2 μ)-Xut1, using glucose as the co-substrate.

Parameter	<i>S. c.</i> XR (2 μ)	<i>S. c.</i> XR (2 μ)-Gal2M	<i>S. c.</i> XR (2 μ)-p427TEF	<i>S. c.</i> XR (2 μ)-Xut1
	Start OD ₆₀₀ /End OD ₆₀₀	3.0/26.7	4.6/26.7	4.4/28.3
μ [1/h] ^a	0.21	0.24	0.27	0.26
Y _{xylitol} [g _{Xol} /g _{Xyl}] ^b	0.79	0.74	0.78	0.65
Y _{co-substrate} [g _{Xol} /g _{Glc}] ^b	0.48	0.44	0.44	0.36
Volumetric xylose uptake rate [g _{Xyl} /(L*h)]	0.65	0.55	0.58	0.50
Specific xylose uptake rate [g _{Xyl} /(g _{CDW} *h)] ^c	0.10	0.08	0.08	0.04
Volumetric xylitol productivity [g _{Xol} /(L*h)]	0.68	0.60	0.56	0.49
Specific xylitol productivity [g _{Xol} /(g _{CDW} *h)] ^c	0.11	0.08	0.08	0.04
Volumetric glucose uptake rate* [g _{Glc} /(L*h)]	1.75	2.85	4.97	3.07
Specific glucose uptake rate* [g _{Glc} /(g _{CDW} *h)] ^b	0.95	1.13	1.84	1.36

^aM.D's on μ were \leq 10%. ^bM.D's on yields were \leq 3 %. ^cM.D's on specific xylose uptake rates and specific xylitol productivities were up to 50 %. *rate determined using data of 0-3 hours. M.D's on specific glucose uptake rates were \leq 30 %. Grey marked row was not used for comparison of the strains because of a too low start OD₆₀₀.

Considering the studies of other working groups, which characterized xylose transport capacities of transporters mainly in yeast strains that lacked endogenous sugar-transporters [17, 25], a study with strains that possess all their natively present transporters seems to be problematic. The small changes in xylose uptake profiles might be overlooked or masked because of the huge influence of the natively expressed transporters, although they should theoretically be saturated with glucose at the beginning of the batch experiment. In order to be able to exclude a masking effect, batch conversions with ethanol instead of glucose as the co-substrate were performed. We expected a suppression of the expression of the native hexose transporters [53] and possibly detectable differences in the specific xylose uptake rates.

The time courses of xylose reduction in the presence of ethanol can be found in Figures 9 and 10. The xylitol yields obtained with the strains *S. c.* XR (2 μ) (0.56 g/g), *S. c.* XR (2 μ)-p427TEF (0.49 g/g), *S. c.* XR (2 μ)-Gal2M (0.45 g/g) and *S. c.* XR (2 μ)-Xut1 (0.44 g/g) were 1.4 to 1.6-fold lower compared to the yields obtained with glucose as the co-substrate (see Table 12), suggesting that glucose is the more efficient co-substrate when fast xylitol production is desired. A moderate decrease in xylitol yields (1.1 to 1.3-fold) was detected in the strains holding two different multiple copy plasmids. Obviously, the existence of a second plasmid negatively influenced the metabolism of the strains *S. c.* XR (2 μ)-p427TEF, *S. c.* XR (2 μ)-Gal2M and *S. c.* XR (2 μ)-Xut1 regarding xylitol production compared to the *S. c.* XR (2 μ) strain. However, biomass formation seemed not to be influenced. This effect was also observable in the experiments with glucose as the co-substrate when considering the differences in the start OD_{600S}.

Comparison of the maximal specific xylose uptake rates (0.08 – 0.07 g/(g_{CDW}*h)) were – within experimental error – the same in all of the four tested strains. Also the Xut1-transporter containing strain showed equal specific xylose uptake and xylitol production rates, which was not the case when glucose was fed as the co-substrate. Interestingly, the use of ethanol instead of glucose did not affect the specific uptake rates and specific productivities of the strains. It is noteworthy to mention, that the medium of the pre-cultures contained glucose. Therefore, an up-regulation of the expression of the native hexose transporters can be suggested. It is questionable if the regression of these native hexose transporters occurred fast enough. If these native hexose transporters were still present when the batch conversions with ethanol as the co-substrate were started probably the masking effect, explained above, could have taken place. To overcome the assumption of a masking effect the *S. c.* IBB10B05 strain was used for further conversion experiments, because this strain is capable of growing on xylose as the sole carbon source.

Table 12: Sugar uptake rates and yields of xylose reduction by *S. c. XR (2μ)*, *S. c. XR (2μ)-Gal2M*, *S. c. XR (2μ)-p427TEF* and *S. c. XR (2μ)-Xut1*, using ethanol as the co-substrate.

Parameter	<i>S. c. XR (2μ)</i>	<i>S. c. XR (2μ)-Gal2M</i>	<i>S. c. XR (2μ)-p427TEF</i>	<i>S. c. XR (2μ)-Xut1</i>
Start OD ₆₀₀ /End OD ₆₀₀	5.3/26.7	5.2/26.7	4.6/21.1	4.4/20.6
μ [1/h] ^a	0.07	0.07	0.06	0.06
Y _{xylitol} [g _{Xol} /g _{Xyl}] ^a	0.56	0.45	0.49	0.44
Y _{co-substrate} [g _{Xol} /g _{EtOH}] ^a	1.11	0.89	1.02	0.92
Volumetric xylose uptake rate [g _{Xyl} /(L*h)]	0.39	0.31	0.32	0.29
Specific xylose uptake rate [g _{Xyl} /(g _{CDW} *h)] ^b	0.08	0.07	0.07	0.08
Volumetric xylitol productivity [g _{Xol} /(L*h)]	0.40	0.33	0.30	0.27
Specific xylitol productivity [g _{Xol} /(g _{CDW} *h)] ^b	0.08	0.07	0.08	0.08

^a M.D's on μ and yields were ≤ 6 %. ^b M.D's on specific xylose uptake rates and specific xylitol productivities were ≤ 50 %.

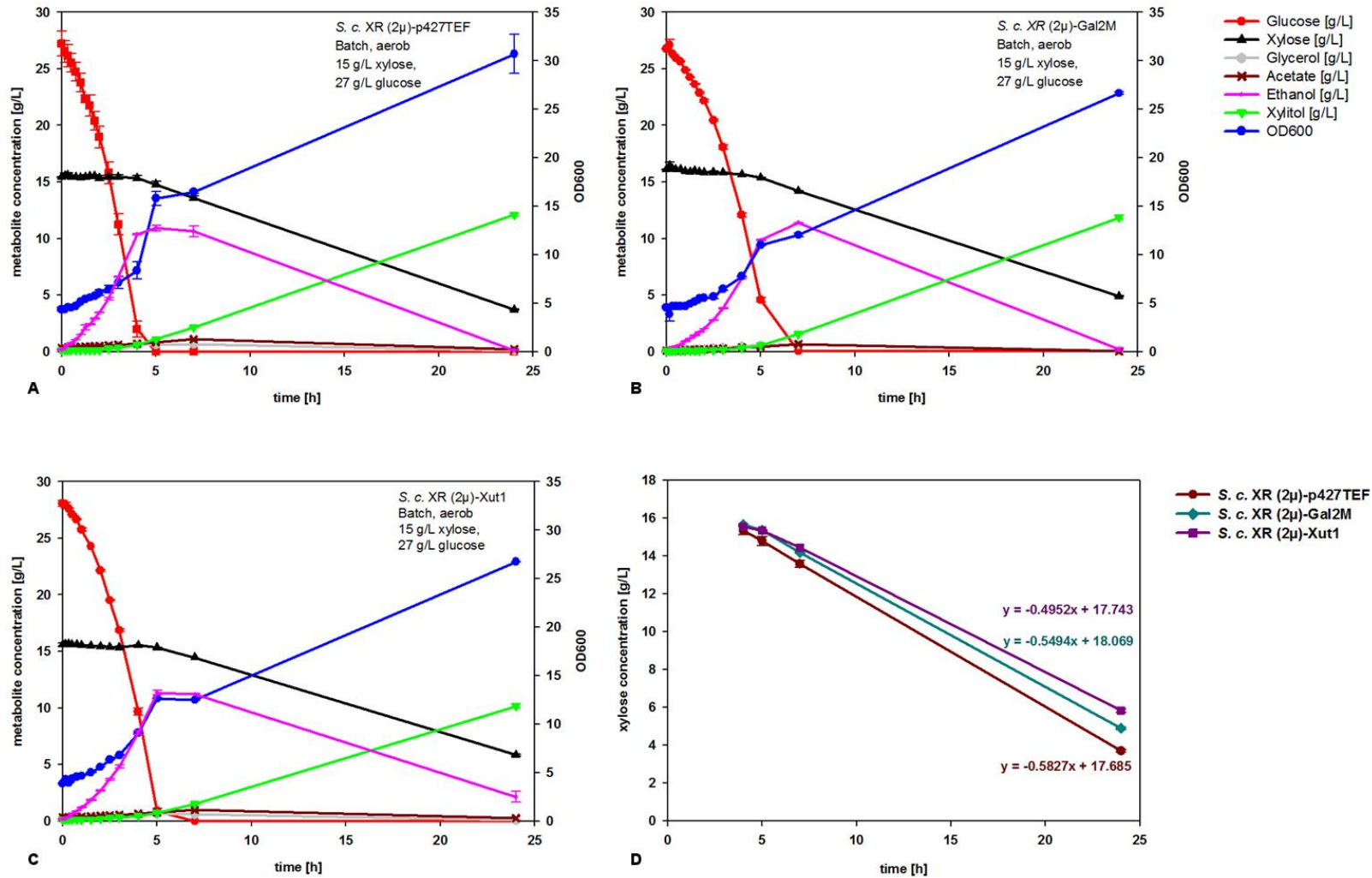


Figure 8: Xylose utilization and product formation during batch conversion in shake flask cultivation of *S. c. XR (2μ)-p427TEF* [A], *S. c. XR (2μ)-Gal2M* [B] and *S. c. XR (2μ)-Xut1* [C], using glucose as the co-substrate. Xylose, xylitol, glycerol, ethanol, acetate and glucose were analyzed by HPLC. Growth was monitored via OD₆₀₀ determination. Xylose uptake profiles and slopes of *S. c. XR (2μ)-p427TEF*, *S. c. XR (2μ)-Gal2M* and *S. c. XR (2μ)-TEF-Xut1* are shown in panel D.

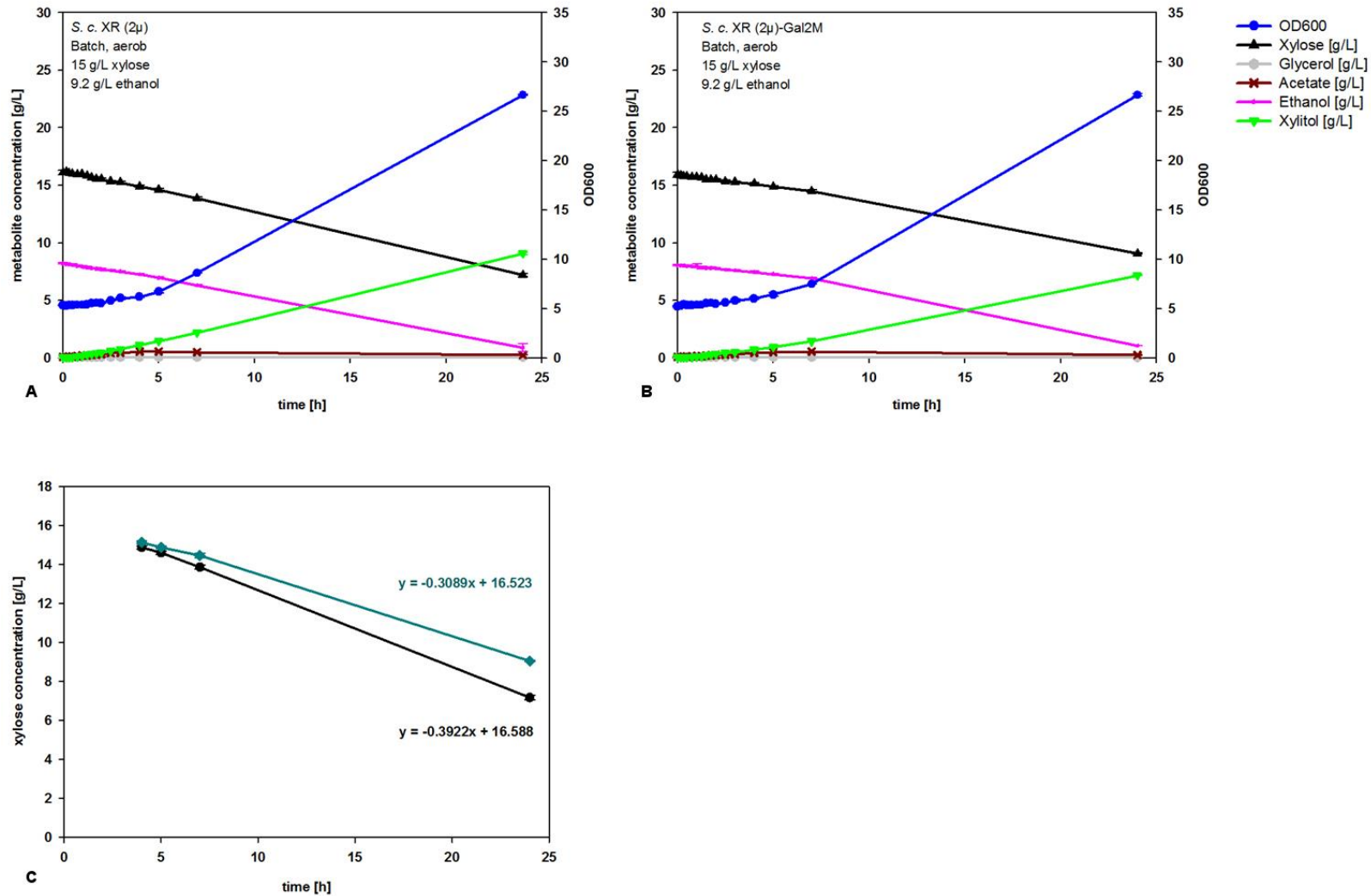


Figure 9: Xylose utilization and product formation during batch conversion in shake flask cultivation of *S. c. XR (2μ)* [A] and *S. c. XR (2μ)-Gal2M* [B], using ethanol as the cosubstrate. Xylose, xylitol, glycerol, acetate and ethanol were analyzed by HPLC. Growth was monitored via OD₆₀₀ determination. Xylose uptake profiles and slopes of *S. c. XR (2μ)* and *S. c. XR (2μ)-Gal2M* are shown in panel C.

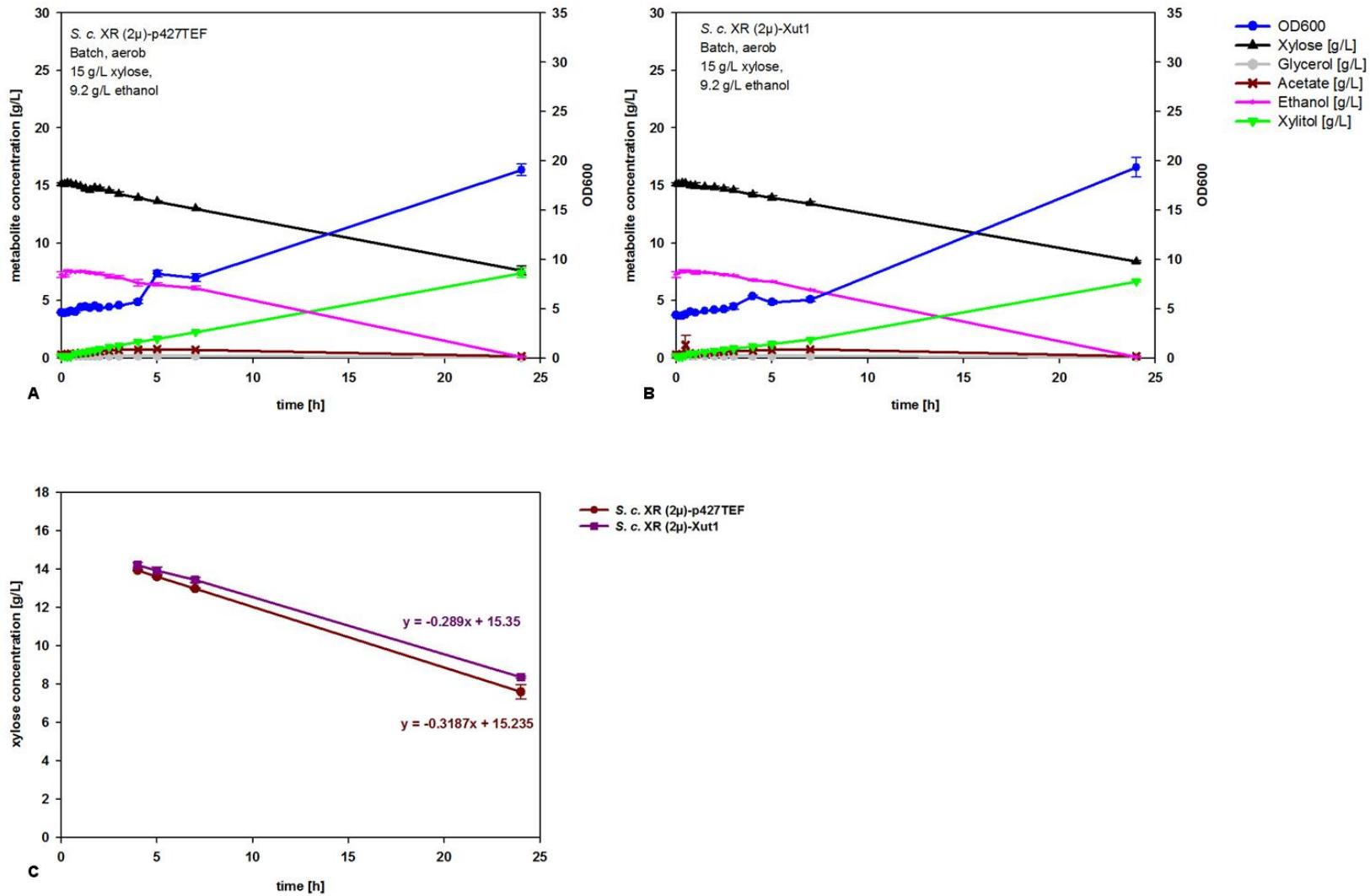


Figure 10: Xylose utilization and product formation during batch conversion in shake flask cultivation of *S. c. XR (2μ)-p427TEF* [A] and *S. c. XR (2μ)-Xut1* [B], using ethanol as the cosubstrate. Xylose, xylitol, glycerol, acetate and ethanol were analyzed by HPLC. Growth was monitored via OD₆₀₀ determination. Xylose uptake profiles and slopes of the *S. c. XR (2μ)-p427TEF* and *S. c. XR (2μ)-XUT1* are shown in panel C.

3.5 The effect of xylose transporter expression in an ethanol-producing high-XR-activity strain

Due to the presence of the xylose-utilization pathway, comprising the enzymes XR, XDH and XKS, the *S. c.* IBB10B05 strain is able to grow on xylose as the sole carbon source. Growth characteristics, xylose uptake behavior and product formation were studied under anaerobic conditions for *S. c.* IBB10B05, *S. c.* IBB10B05-p427TEF, *S. c.* IBB10B05-Gal2M and *S. c.* IBB10B05-Xut1. Representative time courses of xylose utilization and product formation are displayed in Figures 11 and 12. The comparison of strains was pairwise done, due to different start concentrations of the substrate. Xylose conversion employing the *S. c.* IBB10B05 and *S. c.* IBB10B05-Gal2M strains were started with 50 g/L of xylose. For the experiment with *S. c.* IBB10B05-p427TEF and *S. c.* IBB10B05-Xut1 40 g/L of xylose were used.

During the first 22 hours nearly no xylose was consumed. Therefore, data acquired from 27 to 72 hours were used for the determination of the maximal volumetric xylose uptake rates and ethanol productivities. Calculated parameters are summarized in Tables 13 and 14.

Table 13: List of ethanol yields, xylose uptake rates and ethanol productivities of anaerobic batch conversions of the *S. c.* IBB10B05 and *S. c.* IBB10B05-Gal2M strains.

Parameter	<i>S. c.</i> IBB10B05	<i>S. c.</i> IBB10B05-Gal2M
Start OD ₆₀₀ /End OD ₆₀₀	0.2/9.1	0.3/6.3
μ [1/h] ^a	0.06	0.04
Y_{ethanol} [g _{EtOH} /g _{Xyl}] ^a	0.30	0.22
Volumetric xylose uptake rate [g _{Xyl} /(L*h)]	0.66	0.48
Specific xylose uptake rate [g _{Xyl} /(g _{CDW} *h)] ^b	0.54	0.62
Volumetric ethanol productivity [g _{EtOH} /(L*h)]	0.17	0.14
Specific ethanol productivity [g _{EtOH} /(g _{CDW} *h)] ^b	0.14	0.18

^a M.D's on μ and yields were ≤ 5 %. ^b M.D's on specific xylose uptake rates and specific ethanol productivities were up to 46 %.

The ethanol yield obtained with the strain *S. c.* IBB10B05 (0.30 g/g) was 1.4-fold higher than the yield obtained with the *S. c.* IBB10B05-Gal2M (0.22 g/g) strain. Similarly, the product yield of the strain *S. c.* IBB10B05-Xut1 (0.18 g/g) was 1.2-fold decreased compared to the ethanol yield of *S. c.* IBB10B05-

p427TEF (0.21 g/g). The differences in the yields of the *S. c.* IBB10B05 and *S. c.* IBB10B05-Gal2M strains can be reasoned by differences in the growth rates of the respective strains. The transporter-containing strain *S. c.* IBB10B05-Gal2M was growing slower than the transporter-free reference strain and thus less biomass was formed that was capable of xylose reduction (see Figure 11). Additional metabolic pressure, caused by the presence of the p427TEF-Gal2_N376F plasmid, can be mentioned as a reason for decreased cell proliferation.

Considering experimental errors, there were no significant differences in the specific xylose uptake rates of the strains *S. c.* IBB10B05 ($0.54 \text{ g}_{\text{Xyl}}/(\text{g}_{\text{CDW}}*\text{h})$) and *S. c.* IBB10B05-Gal2M ($0.62 \text{ g}_{\text{Xyl}}/(\text{g}_{\text{CDW}}*\text{h})$). Also, specific ethanol productivities were similar ($0.14 \text{ g}_{\text{EtOH}}/(\text{g}_{\text{CDW}}*\text{h})$ and $0.18 \text{ g}_{\text{EtOH}}/(\text{g}_{\text{CDW}}*\text{h})$, respectively). This applies also to specific xylose uptake rates and ethanol productivities of *S. c.* IBB10B05-p427TEF ($0.65 \text{ g}_{\text{Xyl}}/(\text{g}_{\text{CDW}}*\text{h})/0.21 \text{ g}_{\text{EtOH}}/(\text{g}_{\text{CDW}}*\text{h})$) and *S. c.* IBB10B05-Xut1 ($0.69 \text{ g}_{\text{Xyl}}/(\text{g}_{\text{CDW}}*\text{h})/0.23 \text{ g}_{\text{EtOH}}/(\text{g}_{\text{CDW}}*\text{h})$).

Table 14: List of ethanol yields, xylose uptake rates and ethanol productivities of anaerobic batch conversions of the *S. c.* IBB10B05-p427TEF and *S. c.* IBB10B05-Xut1 strains.

Parameter	<i>S. c.</i> IBB10B05- p427TEF	<i>S. c.</i> IBB10B05-XUT1
Start OD ₆₀₀ /End OD ₆₀₀	0.2/5.4	0.2/4.1
μ [1/h] ^a	0.05	0.05
Y_{ethanol} [$\text{g}_{\text{EtOH}}/\text{g}_{\text{Xyl}}$] ^a	0.21	0.18
Volumetric xylose uptake rate [$\text{g}_{\text{Xyl}}/(\text{L}*\text{h})$]	0.34	0.29
Specific xylose uptake rate [$\text{g}_{\text{Xyl}}/(\text{g}_{\text{CDW}}*\text{h})$] ^b	0.65	0.69
Volumetric ethanol productivity [$\text{g}_{\text{EtOH}}/(\text{L}*\text{h})$]	0.11	0.10
Specific ethanol productivity [$\text{g}_{\text{EtOH}}/(\text{g}_{\text{CDW}}*\text{h})$] ^b	0.21	0.23

^a M.D's on μ and yields were ≤ 10 %. ^b M.D's on specific xylose uptake rates and specific ethanol productivities were up to 45 %.

The masking effect of the native hexose transporters should be excludable, due to the ability of all *S. c.* IBB10B05 derived strains of growing solely on xylose as the carbon source. Thus, expression problems of the transporters were strongly assumed (see section 3.6). Furthermore, the assay conditions for the detection of xylose uptake need to be considered. Inability of detecting significant differences in the xylose uptake rates can also result from a too low sensitivity of the assay. Other research groups used

[¹⁴C]-labeled xylose for the uptake experiments [17, 25, 42, 54]. Additionally, the experimental set up of this work generally differs from those of other research groups concerning the xylose concentration that was used [17, 25]. Transport has been speculated to be a problem at lower concentrations, due to the fact that the enzymes in the xylose metabolic pathway have poor affinities to their substrates [24]. Despite this suggestion, in the current study 15 g/L, 40 g/L and 50 g/L of xylose were used, because in lignocellulosic hydrolysates xylose content is rather high. Therefore, a *S. cerevisiae* strain that is capable of effective incorporation and metabolization of high xylose concentrations would be beneficial.

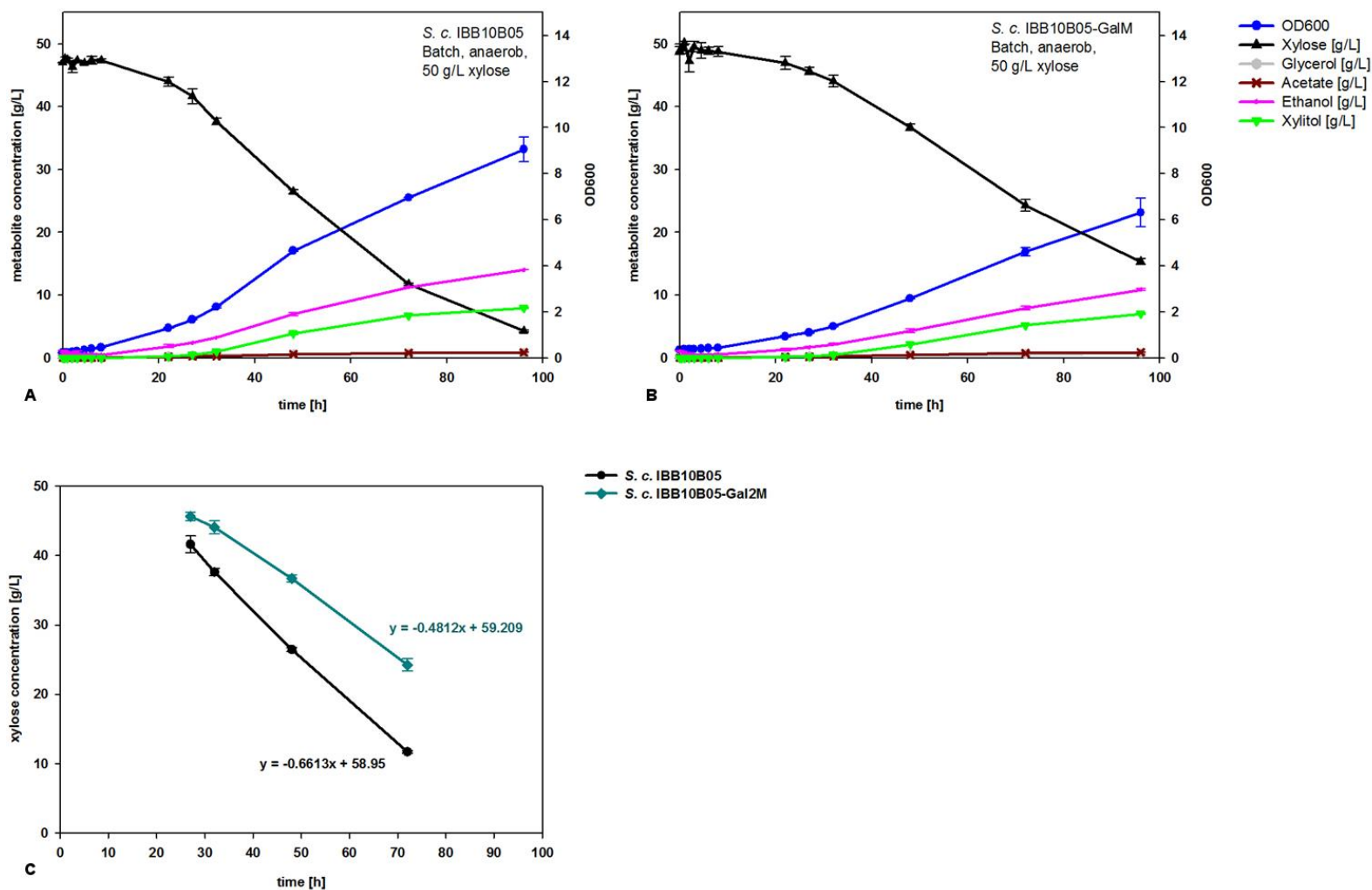


Figure 11: Xylose utilization and product formation during anaerobic batch conversion in airproof, sealed flask cultivation of *S. c. IBB10B05* [A] and *S. c. IBB10B05-Gal2M* [B]. Xylose, xylitol, glycerol, ethanol, acetate and glucose were analyzed by HPLC. Growth was monitored via OD₆₀₀ determination. Xylose uptake profiles and slopes of *S. c. IBB10B05* and *S. c. IBB10B05-Gal2M* are shown in panel C.

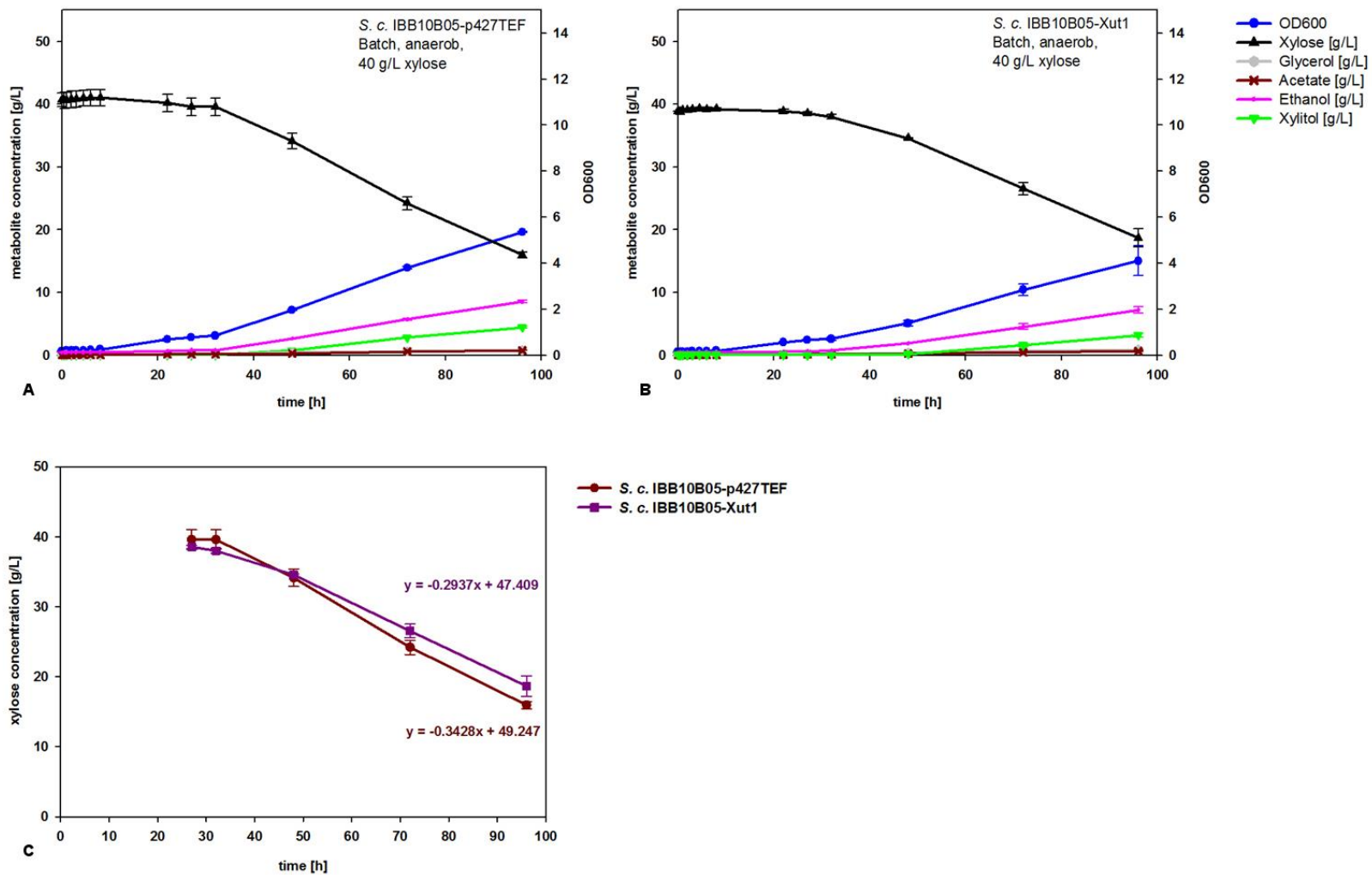


Figure 12: Xylose utilization and product formation during anaerobic batch conversion in airproof, sealed flask cultivation of *S. c. IBB10B05-p427TEF* [A] and *S. c. IBB10B05-Xut1* [B]. Xylose, xylitol, glycerol, ethanol, acetate and glucose were analyzed by HPLC. Growth was monitored via OD₆₀₀ determination. Xylose uptake profiles and slopes of *S. c. IBB10B05-p427TEF* and *S. c. IBB10B05-XUT1* are shown in panel C.

3.6 Analysis of Gal2_N376F transporter expression

To determine if the Gal2_N376F transporter was overexpressed in the respective yeast strains, a Strep-TagII was added C-terminally to the nucleotide sequence of the transporter-gene. Using the p427TEF plasmid, the tagged transporter was expressed in *S. c.* XR (2 μ) and *S. c.* IBB10B05. Liquid cultures were harvested in the mid exponential phase, cells were disrupted and both fractions, crude cell extract (lysate) and cell pellet, were subjected to SDS-PAGE and Western Blot analysis. As a positive control served the strep-tagged glycosyltransferase UGT71A15 which has a size of ~55 kDa. As negative controls served the strains *S. c.* XR (2 μ), *S. c.* IBB10B05, *S. c.* XR (2 μ) Gal2M and *S. c.* IBB10B05-Gal2M. Figure 13 shows the SDS-PAGE gel. Unfortunately, the gel was overloaded by applying 15 μ l of the respective protein samples. As a result protein bands were not clearly separated in the lysate fractions and only a broad smear was detected in the pellet samples. Taken together, from the SDS-PAGE gel it was not possible to verify overexpression of the Gal2_N376F-Strep protein, which has a molecular weight of 64.9 kDa. No bands were visible in the lysate of the *S. c.* IBB10B05-Gal2M-Strep strain, due to a problem with sample loading onto the gel.

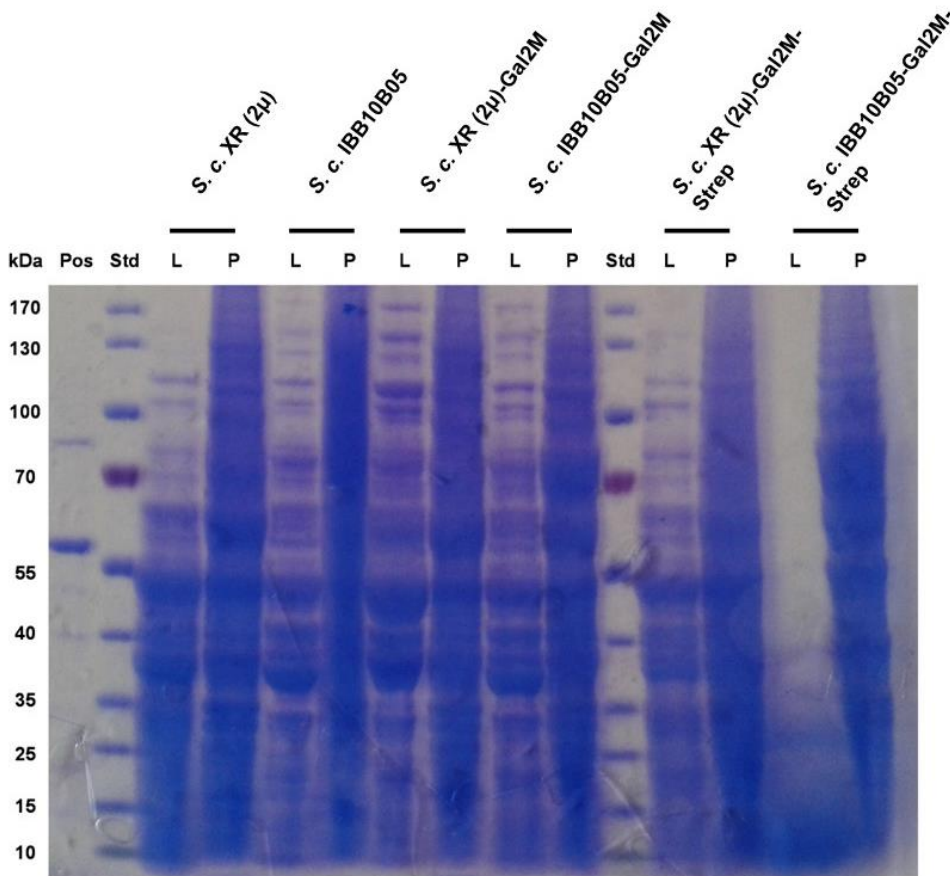


Figure 13: Separation of protein extracts via SDS-PAGE. Pos: positive control Strep-tagged glycosyltransferase UGT71A15 (55 kDa); Std: Page Ruler Prestained Protein Ladder. L: Lysate fractions. P: Pellet fractions.

The Western Blot analysis (Figure 14) resulted in visible bands at the size of ~60 kDa in most of the lysate fractions and all pellet fractions, even in the negative controls where no Strep-Tag has been added. At first sight this indicates unspecific binding of the Strep-Tag antibody to a protein that is mainly present in the cell debris/cell membranes of *S. cerevisiae*. Bands at 64.9 kDa were expected for the Strep-tagged Gal2_N376F transporter in the pellet fractions of the strains that expressed this protein. Considering the anomalous behavior of some proteins in SDS-PAGE, a potential attack by proteases in the cell or during sample processing, together with the minor difference in the size of the detected protein and the molecular weight of the Gal2_N376F transporter, it cannot be totally excluded that the Strep-Tag antibody has bound a sequence in the yeast's native *GAL2* transporter (63.6 kDa). But even if the band at 60 kDa referred to the Gal2 protein, no overexpression of the recombinant mutant was indicated since no significant difference was visible in the thickness of the bands in the control strains and the strains that were supposed to express the transporter. Referring to the obtained results, it seemed as if the Gal2_N376F transporter was not (over)expressed. Possible

reasons can be inappropriate choice of the expression plasmid and/or the promoter. It was shown before that strong overexpression, as it is achieved with the TEF1 promoter [55–58], can be problematic due to non-saturating levels of transcription factors [59]. Additional reasons for detection problems can be incorrect protein folding and/or intracellular protein degradation. However, these factors can mainly be excluded because Gal2 is a *S. cerevisiae* transport protein and should be folded correctly in the native host. Kasahara *et al.* showed that the addition of a C-terminal GFP-Tag to the native Gal2 transporter did not lead to mistrafficking [60], therefore a shorter tag should also not influence the targeting of the transporter to the plasma membrane. Furthermore, the addition of a Strep-Tag did not impair protein expression and detection of several membrane proteins in other hosts such as *E. coli*, *L. lactis* and *A. thaliana* [61]. An additional method to confirm protein expression was shown by the working group of Hector *et al.* They cloned the *At5g59250* and *At5g17010* transporter genes from *A. thaliana* in frame with a C-terminal V5 epitope and used anti-V5-FITC antibodies for the detection of the transporters via Western Blot. The localization of the transporters to the plasma membrane was proofed with fluorescence microscopy [33]. Furthermore, the comparison with the results of other working groups showed that the expression of the Gal2_N376F transporter should be possible. Differences in the choice of the plasmid and the promoter exist: Farwick *et al.* for example used a shortened *HXT7* promoter for the expression of the *GAL2_N376F* transporter gene. If the transporters enhanced the xylose uptake rates no proof of the expression was necessary. Some of the working groups confirmed transcription of each transporter candidate via Real-time Reverse Transcription-PCR measurements [17, 28].

The inconclusive results of the expression-analysis of the Gal2_N376F transporter fit to the conversion experiments. There is no increase in the xylose uptake profile in any of the tested strains, which can be a result of missing protein expression or functionality. The decrease in the xylose uptake profile that was obtained in the strains harboring the *GAL2_N376F* transporter gene compared to the reference strains can eventually be explained by the metabolic burden that is imposed to the microorganism when a protein is overexpressed but subsequently degraded. It is also questionable if the Xut1 transporter was expressed, because the same plasmid p427-TEF was used for the recombinant expression of the transporter. If there was a problem with the promoter (strength) it is likely that the same problem existed for the Xut1 transporter. Additionally, the Xut1 transporter is no native *S. cerevisiae* transporter which may have caused problems with translation, targeting to the membrane or protein folding. The comparison with the work of Jeffries *et al.* showed that the expression of the Xut1 transporter is possible. They cloned the *XUT1* transporter gene under the control of the TDH3 promoter [17].

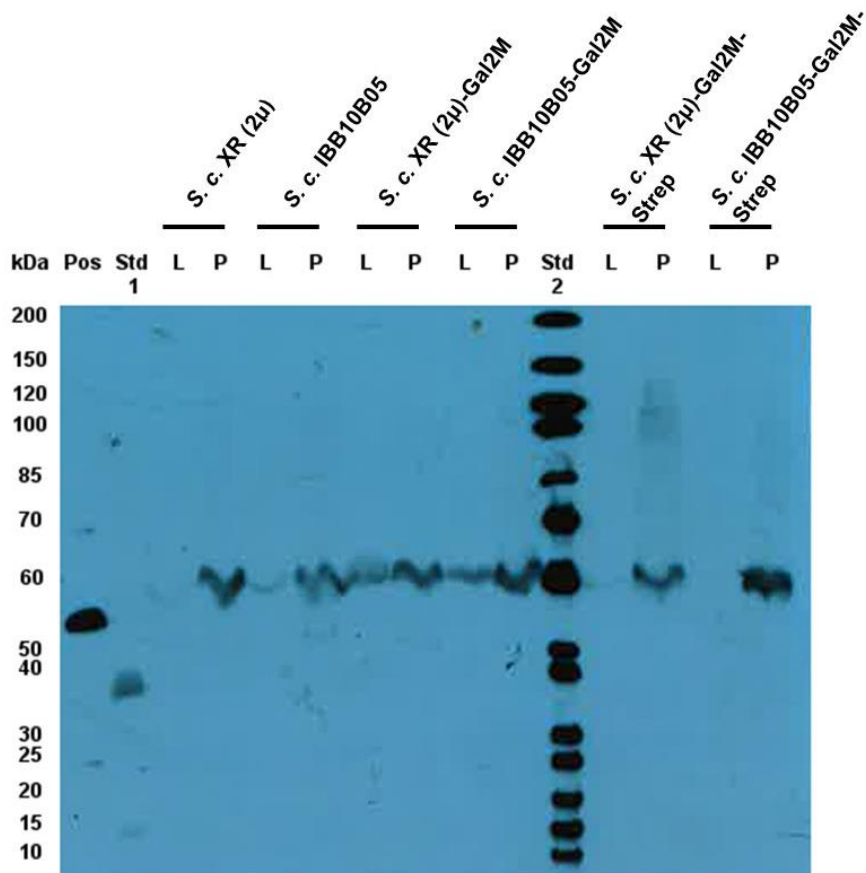


Figure 14: Western Blot analysis of the expression of the Gal2_N376F transporter tagged with a Strep-TagII. Pos: positive control Strep-tagged glycosyltransferase UGT71A15 (55 kDa); Std 1: Page Ruler Prestained Protein Ladder. Std 2: peqGOLD Protein-Marker II (Strep-tagged). L: Lysate fractions. P: Pellet fractions. Bands at ~ 60 kDa are visible in all pellet fractions. In the lysate fractions the bands are pale and no bands are visible in the lysate fractions of *S. c. XR (2μ)-Gal2M-Strep* and *S. c. IBB10B05-Gal2M-Strep*.

4 Conclusion

Lignocellulosic hydrolysates contain mixed sugars (glucose, xylose and arabinose), therefore, the development of a microbial strain capable of fermenting mixed sugars simultaneously is vital for implementing economic conversion processes producing xylitol or biofuels [41]. Although numerous approaches to enhance xylose uptake and to overcome the repression by glucose inhibition have been demonstrated, the simultaneous consumption of these two sugars could not be realized so far with xylose uptake rates comparable to glucose consumption rates [25, 41]. Thus, our approach was to overcome this problem by engineering the xylose uptake capacity of a *S. cerevisiae* strain with the recombinant expression of a xylose specific transporter. In the current study the Gal2_N376F mutant and the Xut1 transporter were used to increase the xylose uptake capacity of the strains *S. c.* XR (g), *S. c.* XR (2 μ) and *S. c.* IBB10B05. Summarizing, the proposed strategy of setting the selected transporters under the control of the strong and constitutive TEF1 promoter did not lead to the expected results. It was not possible to detect a significant difference in maximal specific xylose uptake rates and maximal specific productivities of the constructed strains and the transporter-free controls when co-fermentation of xylose and glucose was investigated. In order to be able to exclude a masking effect of native hexose transporters by the co-substrate glucose, batch conversions with ethanol as the co-substrate and anaerobic conversions with xylose as the sole carbon source were performed. However, it was still impossible to detect significant differences in xylose uptake behavior. Expression analysis of the Gal2_N376F transporter led to inconclusive results. Considering the obtained data from Western Blot analysis, it was impossible to proof the expression of the recombinant protein. If Western Blot analysis gave false negative results and the transporter(s) were actually expressed, they did not increase the xylose uptake capacity of the tested *S. cerevisiae* strains, which possessed all the natively present transporters. Thus, with the applied set-up, we were so far not able to enhance the xylitol or ethanol production in XR or XR-XDH-XKS expressing *S. cerevisiae* strains.

For future work it is necessary to solve the expression problem of the transporters and to find an assay that might overcome detection or sensitivity problems. This might be possible by measuring the internal xylose content when having a strain that does not harbor the XR gene but expresses the additional transporter genes.

5 References

- [1] A. K. Chandel, F. A. F. Antunes, P. V. De Arruda, T. S. S. Milessi, S. S. Silva, and M. G. De, "Dilute Acid Hydrolysis of Agro-Residues for the Depolymerization of Hemicellulose: State-of-the-Art," in *D-Xylitol*, C. Silvio Silverio, da Silva, Anuj Kumar, Ed. Springer Berlin Heidelberg, 2012, pp. 161–191.
- [2] W.-C. Liaw, C.-S. Chen, W.-S. Chang, and K.-P. Chen, "Xylitol production from rice straw hemicellulose hydrolyzate by polyacrylic hydrogel thin films with immobilized *Candida subtropicalis* WF79.," *J. Biosci. Bioeng.*, vol. 105, no. 2, pp. 97–105, Feb. 2008.
- [3] L. Zhu, J. P. O'Dwyer, V. S. Chang, C. B. Granda, and M. T. Holtzapple, "Structural features affecting biomass enzymatic digestibility.," *Bioresour. Technol.*, vol. 99, no. 9, pp. 3817–28, Jun. 2008.
- [4] S. Sun, S. Sun, X. Cao, and R. Sun, "The role of pretreatment in improving the enzymatic hydrolysis of lignocellulosic materials," *Bioresour. Technol.*, vol. 199, pp. 49–58, 2015.
- [5] T. H. (ED. . (Blackie A. & P. Grenby, "Physiological Properties of polyols n comparison with easily metabolisable saccharides," in *Advances in sweeteners*, 1st ed., G. T. H., Ed. Blackie Academic & Professional, an imprint of Chapman & Hall, 1996, pp. 56–77.
- [6] T. B. Granström, K. Izumori, and M. Leisola, "A rare sugar xylitol. Part I: the biochemistry and biosynthesis of xylitol.," *Appl. Microbiol. Biotechnol.*, vol. 74, no. 2, pp. 277–81, Feb. 2007.
- [7] T. B. Granström, K. Izumori, and M. Leisola, "A rare sugar xylitol. Part II: biotechnological production and future applications of xylitol.," *Appl. Microbiol. Biotechnol.*, vol. 74, no. 2, pp. 273–6, Feb. 2007.
- [8] X. Chen, Z.-H. Jiang, S. Chen, and W. Qin, "Microbial and bioconversion production of D-xylitol and its detection and application.," *Int. J. Biol. Sci.*, vol. 6, no. 7, pp. 834–44, Jan. 2010.
- [9] R. S. Rao, C. P. Jyothi, R. S. Prakasham, P. N. Sarma, and L. V. Rao, "Xylitol production from corn fiber and sugarcane bagasse hydrolysates by *Candida tropicalis*," *Bioresour. Technol.*, vol. 97, no. 15, pp. 1974–1978, 2006.
- [10] Z. D. V. L. Mayerhoff, I. C. Roberto, and S. S. Silva, "Xylitol production from rice straw hemicellulose hydrolysate using different yeast strains," *Biotechnol. Lett.*, vol. 19, no. 5, pp. 407–409, 1997.
- [11] A. J. a van Maris, D. a. Abbott, E. Bellissimi, J. van den Brink, M. Kuyper, M. a H. Luttik, H. W. Wisselink, W. A. Scheffers, J. P. van Dijken, and J. T. Pronk, "Alcoholic fermentation of carbon sources in biomass hydrolysates by *Saccharomyces cerevisiae*: Current status," *Antonie van Leeuwenhoek, Int. J. Gen. Mol. Microbiol.*, vol. 90, no. 4, pp. 391–418, 2006.
- [12] B. Peng, Y. Shen, X. Li, X. Chen, J. Hou, and X. Bao, "Improvement of xylose fermentation in

- respiratory-deficient xylose-fermenting *Saccharomyces cerevisiae*,” *Metab. Eng.*, vol. 14, no. 1, pp. 9–18, Jan. 2012.
- [13] B. C. H. Chu and H. Lee, “Genetic improvement of *Saccharomyces cerevisiae* for xylose fermentation,” *Biotechnol. Adv.*, vol. 25, no. 5, pp. 425–41, 2007.
- [14] B. Hahn-Hägerdal, K. Karhumaa, C. Fonseca, I. Spencer-Martins, and M. F. Gorwa-Grauslund, “Towards industrial pentose-fermenting yeast strains,” *Appl. Microbiol. Biotechnol.*, vol. 74, no. 5, pp. 937–53, Apr. 2007.
- [15] T. W. Jeffries, “Engineering yeasts for xylose metabolism,” *Curr. Opin. Biotechnol.*, vol. 17, no. 3, pp. 320–326, 2006.
- [16] N. Q. Meinander and B. Hahn-Hägerdal, “Fed-batch xylitol production with two recombinant *Saccharomyces cerevisiae* strains expressing XYL1 at different levels, using glucose as a cosubstrate: a comparison of production parameters and strain stability,” *Biotechnol. Bioeng.*, vol. 54, no. 4, pp. 391–9, 1997.
- [17] J. B. Thomas William Jeffries, “Sugar Transport Sequences, yeast strains having improved sugar uptake, and methods of use,” Patent No.: US 8,105,811 B2, 2012.
- [18] C. S. Gong, L. F. Chen, M. C. Flickinger, L. C. Chiang, and G. T. Tsao, “Production of Ethanol from d-Xylose by Using d-Xylose Isomerase and Yeasts,” *Appl. Environ. Microbiol.*, vol. 41, no. 2, pp. 430–6, Feb. 1981.
- [19] B. H.-H. J. Hallborn, M.-F. Gorwa, N. Meinander, M. Penttilä, S. Keränen, “The influence of cosubstrate and aeration on xylitol formation by recombinant *Saccharomyces cerevisiae* expressing the XYL1 gene,” *Appl. Microbiol. Biotechnol.*, vol. 42, pp. 326–333, 1994.
- [20] B. Petschacher and B. Nidetzky, “Altering the coenzyme preference of xylose reductase to favor utilization of NADH enhances ethanol yield from xylose in a metabolically engineered strain of *Saccharomyces cerevisiae*,” *Microb. Cell Fact.*, vol. 7, p. 9, Jan. 2008.
- [21] M. Klimacek, E. Kirl, S. Krahulec, K. Longus, V. Novy, and B. Nidetzky, “Stepwise metabolic adaption from pure metabolization to balanced anaerobic growth on xylose explored for recombinant *Saccharomyces cerevisiae*,” *Microb. Cell Fact.*, vol. 13, no. 1, p. 37, 2014.
- [22] B. Petschacher and B. Nidetzky, “Engineering *Candida tenuis* xylose reductase for improved utilization of NADH: Antagonistic effects of multiple side chain replacements and performance of site-directed mutants under simulated in vivo conditions,” *Appl. Environ. Microbiol.*, vol. 71, no. 10, pp. 6390–6393, 2005.
- [23] E. Young, S.-M. Lee, and H. Alper, “Optimizing pentose utilization in yeast: the need for novel tools and approaches,” *Biotechnol. Biofuels*, vol. 3, no. 1, p. 24, Jan. 2010.
- [24] M. Gárdonyi, M. Jeppsson, G. Lidén, M. F. Gorwa-Grauslund, and B. Hahn-Hägerdal, “Control of xylose consumption by xylose transport in recombinant *Saccharomyces cerevisiae*,” *Biotechnol. Bioeng.*, vol. 82, no. 7, pp. 818–24, Jun. 2003.

- [25] A. Farwick, S. Bruder, V. Schadeweg, M. Oreb, and E. Boles, "Engineering of yeast hexose transporters to transport D-xylose without inhibition by D-glucose.," *Proc. Natl. Acad. Sci. U. S. A.*, vol. 111, no. 14, pp. 5159–64, Apr. 2014.
- [26] N. S. Parachin, B. Bergdahl, E. W. J. van Niel, and M. F. Gorwa-Grauslund, "Kinetic modelling reveals current limitations in the production of ethanol from xylose by recombinant *Saccharomyces cerevisiae*," *Metab. Eng.*, vol. 13, no. 5, pp. 508–517, 2011.
- [27] D. Runquist, B. Hahn-Hägerdal, and P. Rådström, "Comparison of heterologous xylose transporters in recombinant *Saccharomyces cerevisiae*," *Biotechnol. Biofuels*, vol. 3, p. 5, Jan. 2010.
- [28] D. Runquist, C. Fonseca, P. Rådström, I. Spencer-Martins, and B. Hahn-Hägerdal, "Expression of the Gxf1 transporter from *Candida intermedia* improves fermentation performance in recombinant xylose-utilizing *Saccharomyces cerevisiae*," *Appl. Microbiol. Biotechnol.*, vol. 82, no. 1, pp. 123–30, Feb. 2009.
- [29] M. J. Leandro, C. Fonseca, and P. Gonçalves, "Hexose and pentose transport in ascomycetous yeasts: An overview," *FEMS Yeast Res.*, vol. 9, no. 4, pp. 511–525, 2009.
- [30] M. E. van der Rest, A. H. Kamminga, A. Nakano, Y. Anraku, B. Poolman, and W. I. L. N. Konings, "The Plasma Membrane of *Saccharomyces cerevisiae* : Structure , Function , and Biogenesis," vol. 59, no. 2, pp. 304–322, 1995.
- [31] J. Du, S. Li, and H. Zhao, "Discovery and characterization of novel d-xylose-specific transporters from *Neurospora crassa* and *Pichia stipitis*," *Mol. Biosyst.*, vol. 6, no. 11, pp. 2150–6, Nov. 2010.
- [32] C. Wang, X. Bao, Y. Li, C. Jiao, J. Hou, Q. Zhang, W. Zhang, W. Liu, and Y. Shen, "Cloning and characterization of heterologous transporters in *Saccharomyces cerevisiae* and identification of important amino acids for xylose utilization," *Metab. Eng.*, vol. 30, pp. 79–88, 2015.
- [33] R. E. Hector, N. Qureshi, S. R. Hughes, and M. a Cotta, "Expression of a heterologous xylose transporter in a *Saccharomyces cerevisiae* strain engineered to utilize xylose improves aerobic xylose consumption.," *Appl. Microbiol. Biotechnol.*, vol. 80, no. 4, pp. 675–84, Sep. 2008.
- [34] S. Katahira, M. Ito, H. Takema, Y. Fujita, T. Tanino, T. Tanaka, H. Fukuda, and A. Kondo, "Improvement of ethanol productivity during xylose and glucose co-fermentation by xylose-assimilating *S. cerevisiae* via expression of glucose transporter Sut1," *Enzyme Microb. Technol.*, vol. 43, no. 2, pp. 115–119, Aug. 2008.
- [35] M. J. Leandro, P. Gonçalves, and I. Spencer-Martins, "Two glucose/xylose transporter genes from the yeast *Candida intermedia*: first molecular characterization of a yeast xylose-H⁺ symporter.," *Biochem. J.*, vol. 395, no. 3, pp. 543–9, May 2006.
- [36] E. Young, A. Poucher, A. Comer, A. Bailey, and H. Alper, "Functional survey for heterologous sugar transport proteins, using *Saccharomyces cerevisiae* as a host.," *Appl. Environ. Microbiol.*, vol. 77, no. 10, pp. 3311–9, May 2011.
- [37] T. Weierstall, C. P. Hollenberg, and E. Boles, "Cloning and characterization of three genes

- (SUT1-3) encoding glucose transporters of the yeast *Pichia stipitis*,” *Mol. Microbiol.*, vol. 31, no. 3, pp. 871–83, Feb. 1999.
- [38] T. Hamacher, J. Becker, M. Gárdonyi, B. Hahn-Hägerdal, and E. Boles, “Characterization of the xylose-transporting properties of yeast hexose transporters and their influence on xylose utilization,” *Microbiology*, vol. 148, no. Pt 9, pp. 2783–8, Sep. 2002.
- [39] T. Jojima, C. a Omumasaba, M. Inui, and H. Yukawa, “Sugar transporters in efficient utilization of mixed sugar substrates: current knowledge and outlook,” *Appl. Microbiol. Biotechnol.*, vol. 85, no. 3, pp. 471–80, Jan. 2010.
- [40] E. M. Young, A. D. Comer, H. Huang, and H. S. Alper, “A molecular transporter engineering approach to improving xylose catabolism in *Saccharomyces cerevisiae*,” *Metab. Eng.*, vol. 14, no. 4, pp. 401–411, 2012.
- [41] S. R. Kim, S.-J. Ha, N. Wei, E. J. Oh, and Y.-S. Jin, “Simultaneous co-fermentation of mixed sugars: a promising strategy for producing cellulosic ethanol,” *Trends Biotechnol.*, vol. 30, no. 5, pp. 274–82, May 2012.
- [42] A. Saloheimo, J. Rauta, O. V Stasyk, A. a Sibirny, M. Penttilä, and L. Ruohonen, “Xylose transport studies with xylose-utilizing *Saccharomyces cerevisiae* strains expressing heterologous and homologous permeases,” *Appl. Microbiol. Biotechnol.*, vol. 74, no. 5, pp. 1041–52, Apr. 2007.
- [43] A. Maier, B. Vo, E. Boles, and F. Fuhrmann, “Characterisation of glucose transport in *Saccharomyces cerevisiae* with plasma membrane vesicles (countertransport) and intact cells Gal2 transporters,” vol. 2, pp. 539–550, 2002.
- [44] S. Krahulec, B. Petschacher, M. Wallner, K. Longus, M. Klimacek, and B. Nidetzky, “Fermentation of mixed glucose-xylose substrates by engineered strains of *Saccharomyces cerevisiae*: role of the coenzyme specificity of xylose reductase, and effect of glucose on xylose utilization,” *Microb. Cell Fact.*, vol. 9, p. 16, 2010.
- [45] M. Jeppsson, O. Bengtsson, K. Franke, H. Lee, B. Hahn-Hägerdal, and M. F. Gorwa-Grauslund, “The expression of a *Pichia stipitis* xylose reductase mutant with higher KM for NADPH increases ethanol production from xylose in recombinant *Saccharomyces cerevisiae*,” *Biotechnol. Bioeng.*, vol. 93, no. 4, pp. 665–673, 2006.
- [46] R. Kratzer, S. Egger, and B. Nidetzky, “Integration of enzyme, strain and reaction engineering to overcome limitations of baker’s yeast in the asymmetric reduction of alpha-keto esters,” *Biotechnol. Bioeng.*, vol. 101, no. 5, pp. 1094–101, Dec. 2008.
- [47] B. Agindotan and K. L. Perry, “DNA MODIFYING ENZYMES Gibson Assembly™ Cloning Kit,” *Phytopathology*, vol. 97, no. 1, pp. 119–27, 2007.
- [48] R. D. Gietz and R. a Woods, “Transformation of yeast by lithium acetate/single-stranded carrier DNA/polyethylene glycol method,” *Methods Enzymol.*, vol. 350, no. 2001, pp. 87–96, Jan. 2002.
- [49] H. A. Riezman, “Rapid protein extraction from *Saccharomyces cerevisiae*,” *Yeast*, vol. 10, pp. 1305–1310, 1994.

- [50] S. M. Pratter, T. Eixelsberger, and B. Nidetzky, "Systematic strain construction and process development: Xylitol production by *Saccharomyces cerevisiae* expressing *Candida tenuis* xylose reductase in wild-type or mutant form," *Bioresour. Technol.*, vol. 198, pp. 732–738, 2015.
- [51] S. Ozcan and M. Johnston, "Three different regulatory mechanisms enable yeast hexose transporter (HXT) genes to be induced by different levels of glucose.," *Mol. Cell. Biol.*, vol. 15, no. 3, pp. 1564–1572, 1995.
- [52] M. Sedlak and N. W. Y. Ho, "Characterization of the effectiveness of hexose transporters for transporting xylose during glucose and xylose co-fermentation by a recombinant *Saccharomyces* yeast.," *Yeast*, vol. 21, no. 8, pp. 671–84, Jun. 2004.
- [53] M. Chandler, G. A. Stanley, P. Rogers, and P. Chambers, "A genomic approach to defining the ethanol stress response in the yeast *Saccharomyces cerevisiae*," vol. 54, no. 4, pp. 427–454, 2004.
- [54] W.-J. Lee, M.-D. Kim, Y.-W. Ryu, L. F. Bisson, and J.-H. Seo, "Kinetic studies on glucose and xylose transport in *Saccharomyces cerevisiae*," *Appl. Microbiol. Biotechnol.*, vol. 60, no. 1–2, pp. 186–91, Oct. 2002.
- [55] D. Mumberg, R. Müller, and M. Funk, "Yeast vectors for the controlled expression of heterologous proteins in different genetic backgrounds.," *Gene*, vol. 156, no. 1, pp. 119–22, Apr. 1995.
- [56] E. Nevoigt, J. Kohnke, C. R. Fischer, H. Alper, U. Stahl, and G. Stephanopoulos, "Engineering of promoter replacement cassettes for fine-tuning of gene expression in *Saccharomyces cerevisiae*," *Appl. Environ. Microbiol.*, vol. 72, no. 8, pp. 5266–5273, 2006.
- [57] J. Sun, Z. Shao, H. Zhao, N. Nair, F. Wen, J.-H. Xu, and H. Zhao, "Cloning and characterization of a panel of constitutive promoters for applications in pathway engineering in *Saccharomyces cerevisiae*," *Biotechnol. Bioeng.*, vol. 109, no. 8, pp. 2082–2092, 2012.
- [58] V. Nacken, T. Achstetter, and E. Degryse, "Probing the limits of expression levels by varying promoter strength and plasmid copy number in *Saccharomyces cerevisiae*," *Gene*, vol. 175, no. 1–2, pp. 253–260, 1996.
- [59] S. M. Baker, S. a Johnston, J. E. Hopper, and J. a Jaehning, "Transcription of multiple copies of the yeast *GAL7* gene is limited by specific factors in addition to *GAL4*," *Mol. Gen. Genet.*, vol. 208, no. 1–2, pp. 127–134, 1987.
- [60] T. Kasahara and M. Kasahara, "Three Aromatic Amino Acid Residues Critical for Galactose Transport in Yeast *Gal2* Transporter," *J. Biol. Chem.*, vol. 275, no. 6, pp. 4422–4428, Feb. 2000.
- [61] F. Bernaudat, A. Frelet-Barrand, N. Pochon, S. Dementin, P. Hivin, S. Boutigny, J.-B. Rioux, D. Salvi, D. Seigneurin-Berny, P. Richaud, J. Joyard, D. Pignol, M. Sabaty, T. Desnos, E. Pebay-Peyroula, E. Darrouzet, T. Vernet, and N. Rolland, "Heterologous Expression of Membrane Proteins: Choosing the Appropriate Host," *PLoS One*, vol. 6, no. 12, p. e29191, 2011.

6 Appendix

6.1 DNA and Protein Sequences

The accession numbers of the genes expressed in this work are found in Table 15.

Table 15: Accession numbers of the *GAL2* and the *XUT1* gene

Gene	Accession number	Length [bp]
<i>Gal2</i>	P13181	574
<i>XUT1</i>	A3LY10	566

DNA Sequence of *XUT1* flanked with 5'-*Bam*HI and 3'-*Xma*I

Restriction sites are marked in grey and the start codon is marked in yellow.

```
GGATCCATGCACGGTGGTGGTGACGGTAACGATATCACAGAAATTATTGCAGCCAGACGTCTCCAGATCGC
TGGTAAGTCTGGTGTGGCTGGTTTAGTCGCAAACCTCAAGATCTTTCTTCATCGCAGTCTTTGCATCTCTTG
GTGGATTGGTCTACGGTTACAATCAAGGTATGTTCCGGTCAAATTTCCGGTATGTACTCATTCTCCAAAGCT
ATTGGTGTGAAAAGATTCAAGACAATCCTACTTTGCAAGGTTTGTGACTTCTATTCTTGAACCTGGTGC
CTGGGTGGTGTCTTGATGAACGGTTACATTGCTGATAGATTGGGTCGTAAGAAGTCAGTTGTTGTCCGGTG
TTTTCTTCTTCTTCATCGGTGTCATTGTACAAGCTGTTGCTCGTGGTGGTAACTACGACTACATCTTAGGT
GGTAGATTTGTCGTCGGTATTGGTGTGGGTATTCTTTCTATGGTTGTGCCATTGTACAATGCTGAAGTTTC
TCCACCAGAAATTCGTGGTTCTTTGGTTGCTTTGCAACAATTGGCTATTACTTTCCGGTATTATGATTTCTT
ACTGGATTACCTACGGTACCAACTACATTGGTGGTACTGGCTCTGGTCAAAGTAAAGCTTCTTGGTTGGTT
CCTATTTGTATCCAATTGGTTCCAGCTTTGCTCTTGGGTGTTGGTATCTTCTTCATGCCTGAGTCTCCAAG
ATGGTTGATGAACGAAGACAGAGAAGACGAATGTTTGTCCGTTCTTTCCAACCTGCGTTCCTTGAGTAAGG
AAGATACTCTTGTTCAAATGGAATTCCTTGAATGAAGGCACAAAAGTTGTTTCGAAAGAGAACTTTCTGC
AAAGTACTTCCCTCACCTCCAAGACGGTTCTGCCAAGAGCAACTTCTTGATTGGTTTCAACCAATACAAGT
CCATGATTACTCACTACCAACCTTCAAGCGTGTGTCAGTTGCCTGTTAATTATGACCTTCCAACAATGG
ACTGGTGTAACTTCATCTTGTACTATGCTCCATTCATCTTCAGTTCTTTAGGTTTGTCTGGAAACACCAT
TTCTCTTTTAGCTTCTGGTGTGTCGGTATCGTCATGTTCCCTTGCTACCATTCCAGCTGTTCTTTGGGTCTGA
CAGACTTGGTAGAAAGCCAGTTTTGATTTCCGGTGCCATTATCATGGGTATTTGTCACTTTGTTGTGGCTG
CAATCTTAGGTCAGTTCGGTGGTAACTTTGTCAACCACTCCGGTGCTGGTGGGTTGCTGTTGTCTTCGTT
```

TGGATTTTCGCTATCGGTTTCGGTACTCTTGGGGTCCATGTGCTTGGGTCCTTGTTGCCGAAGTCTTCCCA
TTGGGTTTGCCTGCTAAGGGTGTCTTCTATCGGTGCCTCTTCTAACTGGTTGAACAACTTCGCTGTCGCCAT
GTCTACCCAGATTTTGTGCTAAGGCTAAGTTCGGTGCCTTACATTTTCTTAGGTTTGTATGTGATTTTTCG
GTGCCGCATACGTTCAATTCTTCTGTCCAGAACTAAGGGTTCGTACCTTGGAAGAAATGATGAACTTTTC
GGTGACACCTCTGGTACTTCCAAGATGGAAAAGGAAATCCATGAGCAAAGCTTAAGGAAGTTGGTTTGC
TTCAATTGCTCGGTGAAGAAAATGCTTCTGAATCCGAAAACAGCAAGGCTGATGTCTACCACGTTGAAAAA
TAACCCGGG

DNA Sequence of *Gal2_N376F* flanked with 5'-*Xma*I and 3'-*Eco*RI

Restriction sites are marked in grey, start codon is marked in yellow and the N376F mutation is marked green.

CCCGGGATGCGCAGTTGAGGAGAACAATATGCCTGTTGTTTCACAGCAACCCCAAGCTGGTGAAGACGTGAT
CTCTTCACTCAGTAAAGATTTCCATTTAAGCGCACAACTCAAAGTATTCTAATGATGAATTGAAAGCCG
GTGAGTCAGGGTCTGAAGGCTCCCAAAGTGTTCCTATAGAGATACCCAAGAAGCCCATGTCTGAATATGTT
ACCGTTTCCTTGCTTTGTTTGTGTGTTGCCTTCGGCGGCTTCATGTTTGGCTGGGATACCGTACTATTTCT
GGGTTTGTGTCCAAACAGACTTTTTGAGAAGGTTGGTATGAAACATAAGGATGGTACCCACTATTTGTC
AAACGTCAGAACAGGTTAATCGTCGCCATTTTCAATATTGGCTGTGCCTTTGGTGGTATTATACTTTCCA
AAGGTGGAGATATGTATGGCCGTA AAAAGGGTCTTCGATTGTCGTCTCGGTTTATATAGTTGGTATTATC
ATTCAAATTGCCTCTATCAACAAGTGGTACCAATATTTCAATTGGTAGAATCATATCTGGTTTGGGTGTCGG
CGGCATCGCCGTCTTATGTCCTATGTTGATCTCTGAAATTGCTCCAAAGCACTTGAGAGGCACACTAGTTT
CTTGTTATCAGCTGATGATTACTGCAGGTATCTTTTTGGGCTACTGTACTAATTACGGTACAAAGAGCTAT
TCGAACTCAGTTCAATGGAGAGTTCATTAGGGCTATGTTTCGCTTGGTCATTATTTATGATTGGCGCTTT
GACGTTAGTTCTGAATCCCCACGTTATTTATGTGAGGTGAATAAGGTAGAAGACGCCAAGCGTTCCATTG
CTAAGTCTAACAAGGTGTCACCAGAGGATCCTGCCGTCCAGGCAGAGTTAGATCTGATCATGGCCGGTATA
GAAGCTGAAAACTGGCTGGCAATGCGTCCTGGGGGAATTATTTTCCACCAAGACCAAAGTATTTCAACG
TTTGTTGATGGGTGTGTTTGTTCAAATGTTCCAACAATTAACCGGTAACAATTATTTTTTCTACTACGGTA
CCGTTATTTCAAGTCAGTTGGCCTGGATGATTCTTTGAAACATCCATTGTCATTGGTGTAGTCTTCTTT
GCCTCCACTTTCTTTAGTTTGTGGACTGTGCAAACTTGGGACATCGTAAATGTTTACTTTTGGGCGCTGC
CACTATGATGGCTTGTATGGTCATCTACGCCTCTGTTGGTGTTACTAGATTATATCCTCACGGTAAAAGCC
AGCCATCTTCTAAAGGTGCCGGTAACTGTATGATTGTCTTTACCTGTTTTTATATTTTCTGTTATGCCACA
ACCTGGGCGCCAGTTGCCTGGGTGTCATCACAGCAGAATCATTTCCACTGAGAGTCAAGTCGAAATGTATGGC
GTTGGCCTCTGCTTCCAATTGGGTATGGGGTCTTGATTGCATTTTTTACCCCATTCATCACATCTGCCAT
TAACTTCTACTACGGTTATGTCTTCATGGGCTGTTTGGTTGCCATGTTTTTTTATGTCTTTTTCTTTGTTC

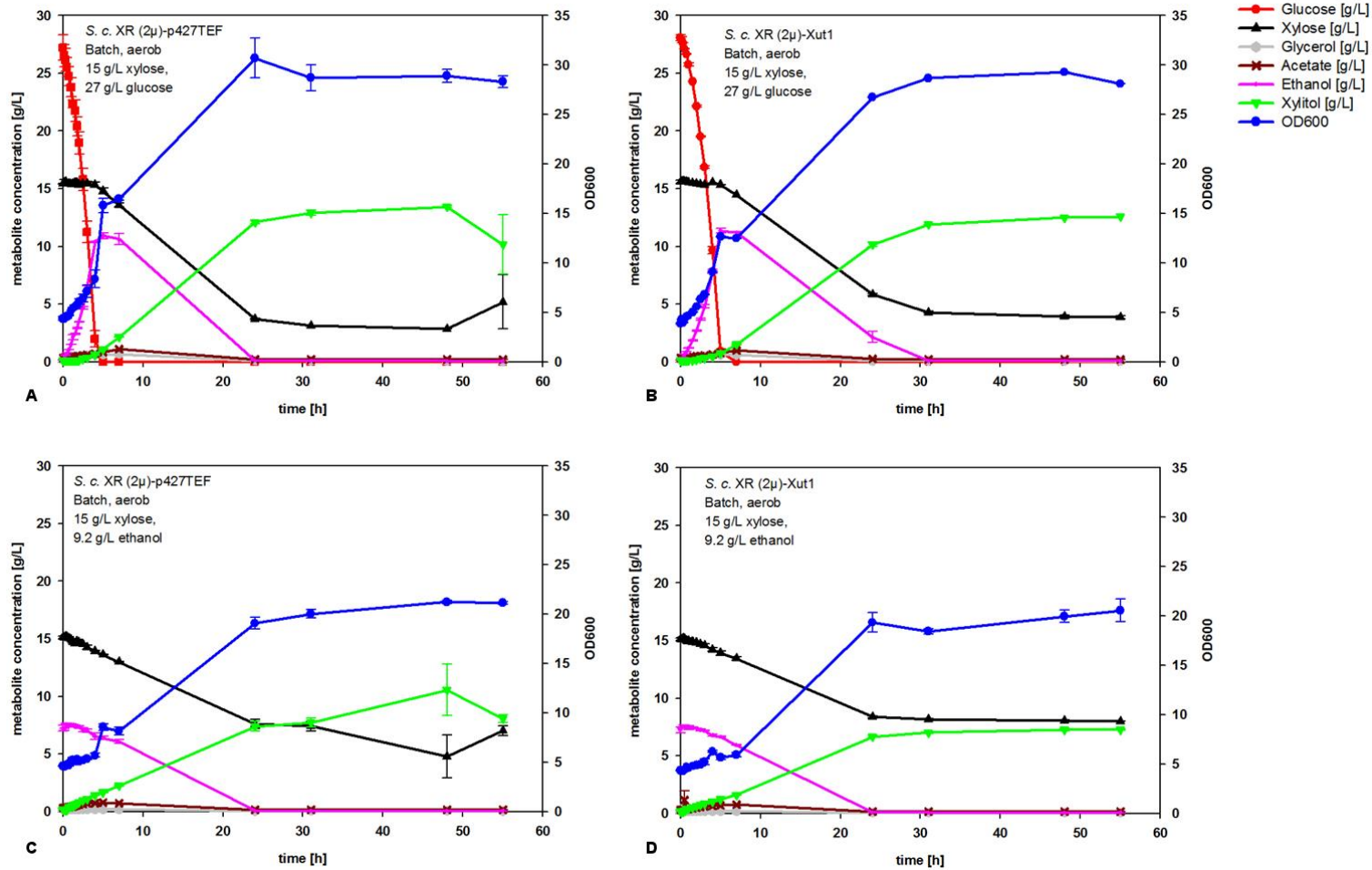
CAGAACTAAAGGCCTATCGTTAGAAGAAATTCAAGAATTATGGGAAGAAGGTGTTTTACCTTGGAATC
TGAAGGCTGGATTCCCTTCATCCAGAAGAGGTAATAATTACGATTTAGAGGATTTACAACATGACGACAAA
CCGTGGTACAAGGCCATGCTAGAATAAGAATTC

**DNA Sequence of *Gal2_N376F* with the C-terminally attached Strep-Tag sequence flanked with 5'-*XmaI*
and 3'-*EcoRI***

Restriction sites are marked in grey, start codon is marked in yellow, the N376F mutation is marked green and the Strep-Tag sequence is marked in pink.

CCCGGGATGGCAGTTGAGGAGAACAATATGCCTGTTGTTTCACAGCAACCCCAAGCTGGTGAAGACGTGAT
CTCTTCACTCAGTAAAGATTCCCATTTAAGCGCACAATCTCAAAGTATTCTAATGATGAATTGAAAGCCG
GTGAGTCAGGGTCTGAAGGCTCCCAAAGTGTTCCCTATAGAGATACCCAAGAAGCCCATGTCTGAATATGTT
ACCGTTTCCTTGCTTTGTTTGTGTGTTGCCTTCGGCGGCTTCATGTTTGGCTGGGATACCGGTACTATTTCT
GGGTTTGTGTCCAAACAGACTTTTTGAGAAGGTTTGGTATGAAACATAAGGATGGTACCCACTATTTGTC
AAACGTCAGAACAGGTTTAATCGTCGCCATTTTCAATATTGGCTGTGCCTTTGGTGGTATTATACTTTCCA
AAGGTGGAGATATGTATGGCCGTAAAAAGGGTCTTTCGATTGTCGTCTCGGTTTATATAGTTGGTATTATC
ATTCAAATTGCCTCTATCAACAAGTGGTACCAATATTTCAATTGGTAGAATCATATCTGGTTTGGGTGTCGG
CGGCATCGCCGTCTTATGTCCTATGTTGATCTCTGAAATTGCTCCAAAGCACTTGAGAGGCACACTAGTTT
CTTGTTATCAGCTGATGATTACTGCAGGTATCTTTTTGGGCTACTGTACTAATTACGGTACAAAGAGCTAT
TCGAACTCAGTTCAATGGAGAGTTCCATTAGGGCTATGTTTCGCTTGGTCATTATTTATGATTGGCGCTTT
GACGTTAGTTCTGAATCCCCACGTTATTTATGTGAGGTGAATAAGGTAGAAGACGCCAAGCGTTCCATTG
CTAAGTCTAACAAGGTGTCACCAGAGGATCCTGCCGTCCAGGCAGAGTTAGATCTGATCATGGCCGGTATA
GAAGCTGAAAACTGGCTGGCAATGCGTCCTGGGGGAATTATTTCCACCAAGACCAAAGTATTTCAACG
TTTGTTGATGGGTGTGTTTGTTCAAATGTTCCAACAATTAACCGGTAACAATTATTTTTCTACTACGGTA
CCGTTATTTCAAGTCAGTTGGCCTGGATGATTCCTTTGAAACATCCATTGTCATTGGTGTAGCTTTCCTTT
GCCTCCACTTTCTTTAGTTTGTGGACTGTGAAAACCTGGGACATCGTAAATGTTTACTTTTGGGCGCTGC
CACTATGATGGCTTGTATGGTCATCTACGCCTCTGTTGGTGTACTAGATTATATCCTCACGGTAAAAGCC
AGCCATCTTCTAAAGGTGCCGGTAACTGTATGATTGTCTTTACCTGTTTTATATTTTCTGTTATGCCACA
ACCTGGGCGCCAGTTGCCTGGGTCATCACAGCAGAATCATTCCCACTGAGAGTCAAGTCGAAATGTATGGC
GTTGGCCTCTGCTTCCAATTGGGTATGGGGTCTTGGATTGCATTTTTACCCCATTCATCACATCTGCCAT
TAACTTCTACTACGGTTATGTCTTCATGGGCTGTTTGGTTGCCATGTTTTTTTATGTCTTTTTCTTTGTTT
CAGAACTAAAGGCCTATCGTTAGAAGAAATTCAAGAATTATGGGAAGAAGGTGTTTTACCTTGGAATC
TGAAGGCTGGATTCCCTTCATCCAGAAGAGGTAATAATTACGATTTAGAGGATTTACAACATGACGACAAA
CCGTGGTACAAGGCCATGCTAGAAATCAGCTTGGTCACATCCTCAGTTTCGAGAAATAAGAATTC

6.2 Batch Conversion Diagrams



6.3 Instruments and devices

Centrifuges:

Centrifuge “Eppifuge” 5415R: Eppendorf AG, Hamburg, Germany

Centrifuge 5804R “tube 15 mL, 50 mL”: Eppendorf AG, Hamburg, Germany

Centrifuge Sorvall Evolution RC: Thermo Fisher Scientific, Waltham, USA

Thermocycler:

iCycler thermal cycler (serial number 582BR): Bio-Rad Laboratories Ges.m.b.H, Vienna, Austria

MyCycler™ thermal cycler (serial number 578BR): Bio-Rad Laboratories Ges.m.b.H, Vienna, Austria

AB 2720 Thermo Cycler: Applied Biosystems®, Vienna, Austria

Thermomixer:

Thermomixer comfort: Eppendorf AG, Hamburg, Germany

Shaker:

Certomat® BS-1: Sartorius Stedim Austria GmbH, Vienna, Austria

Pilot-Shaker: Adolf Küher AG, Basel, Switzerland

Spectrophotometer:

DU 800 Spectrophotometer: Beckman Coulter Inc, Fullerton, CA, US

DeNovix DS-11 UV-Vis Spectrophotometer “Nanodrop”: DeNovix Inc., Wilmington, USA

HPLC:

LaChrom HPLC system: Merck – Hitachi LaChrom (Darmstadt, Germany - San Jose, USA)

- Pump L-7100
- RI detector L-7490
- Autosampler L-7250
- HPLC system manager software D-7000

Shimadzu HPLC system: Shimadzu Scientific Instruments, Columbia, U.S.A.

- Pump LC-20AD
- RI detector 10-A
- Autosampler SIL-20AC
- Labsolutions software – LCMS 2020

Additional Instruments and devices:

Micro Pulser™ (electroporation device): Bio-Rad Laboratories Ges.m.b.H, Vienna, Austria

SONOREX DIGITC DT255 Ultrasonic bath: BANDELIN electronic GmbH & Co. KG, Berlin, Germany

pH meter 691: Metrohm AG, Herisau, Switzerland

pH meter inoLab 720: WTW Wissenschaftlich-Technische Werkstätten GmbH, Weilheim, Germany